Imaging Geospace: Providing Critical Understanding of Earth's Atmosphere-Ionosphere System

Thomas J. Immel

Space Sciences Laboratory

University of California Berkeley

With thanks to Scott England, Stephen Mende, Jeff Forbes, Xiaoli Zhang, Maura Hagan, and John Foster

2008 CEDAR Workshop

2-D imaging of Earth's upper-atmospheric airglow emissions was first achieved with a lunar-based imager during Apollo 16.

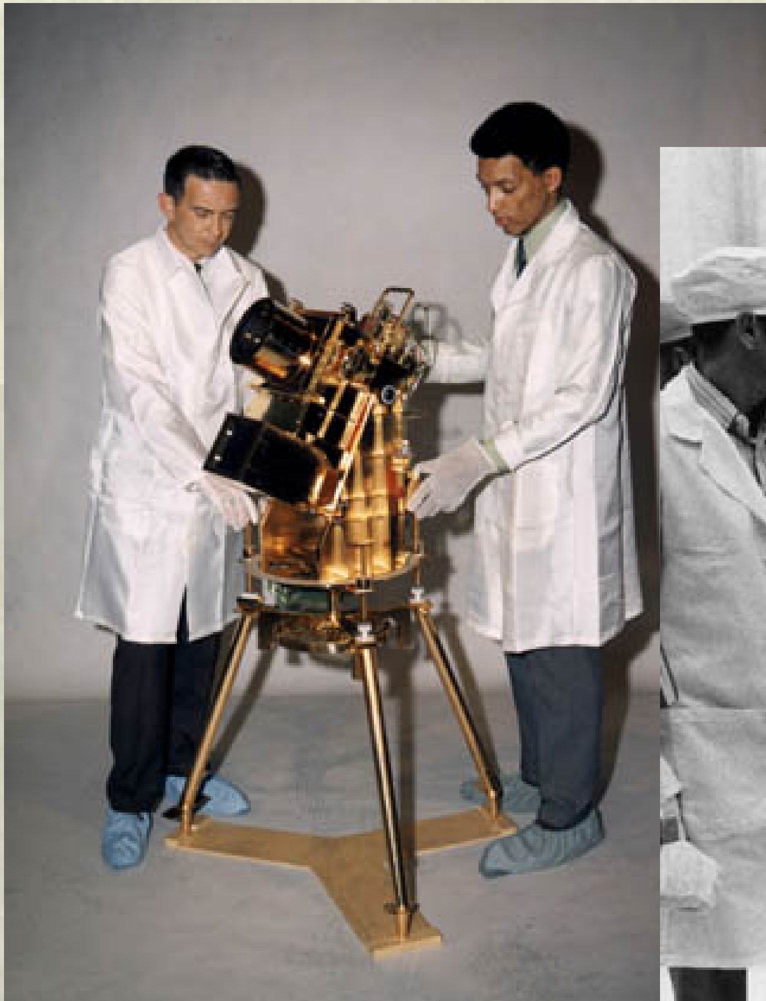

2-D imaging of Earth’s upper-atmospheric airglow emissions was first achieved with a lunar-based imager during Apollo 16.

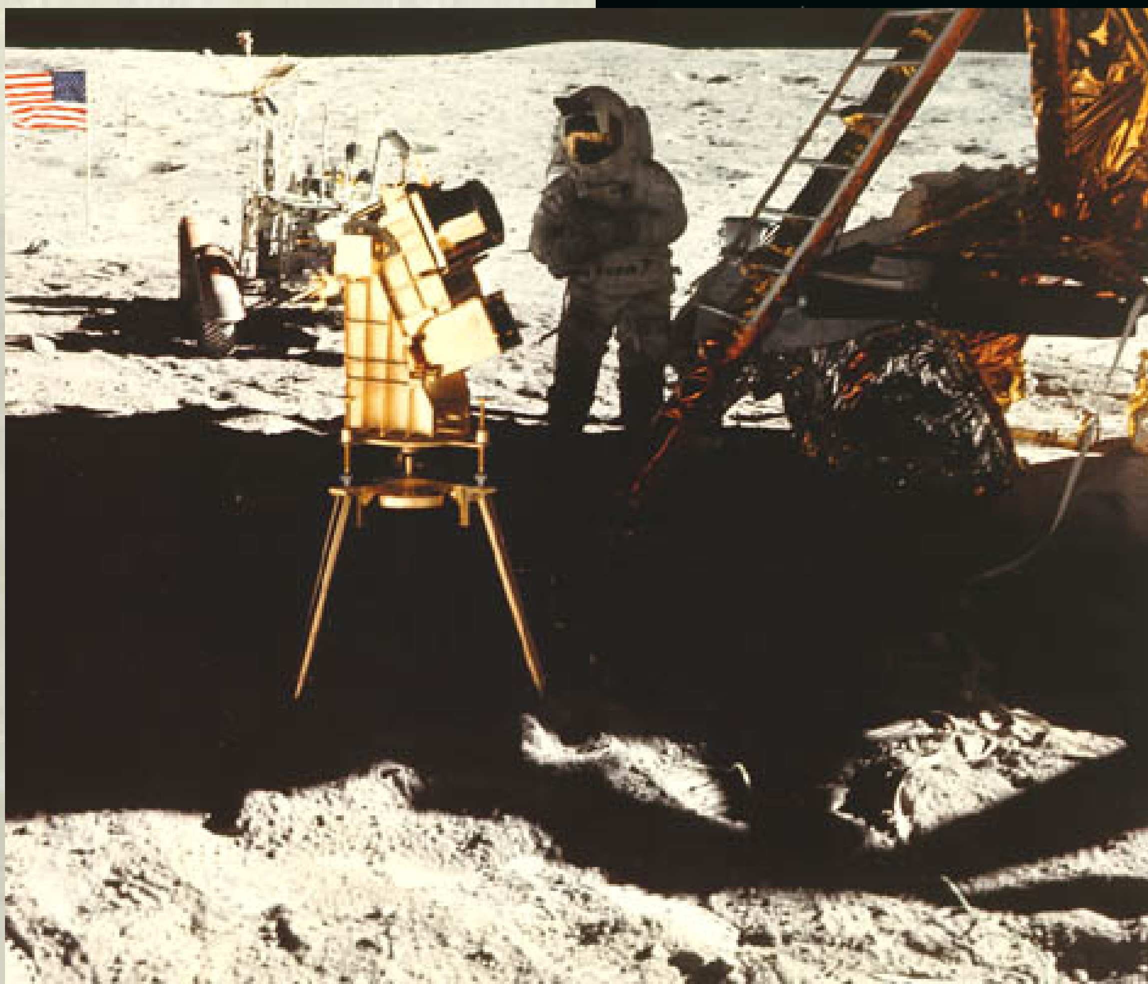

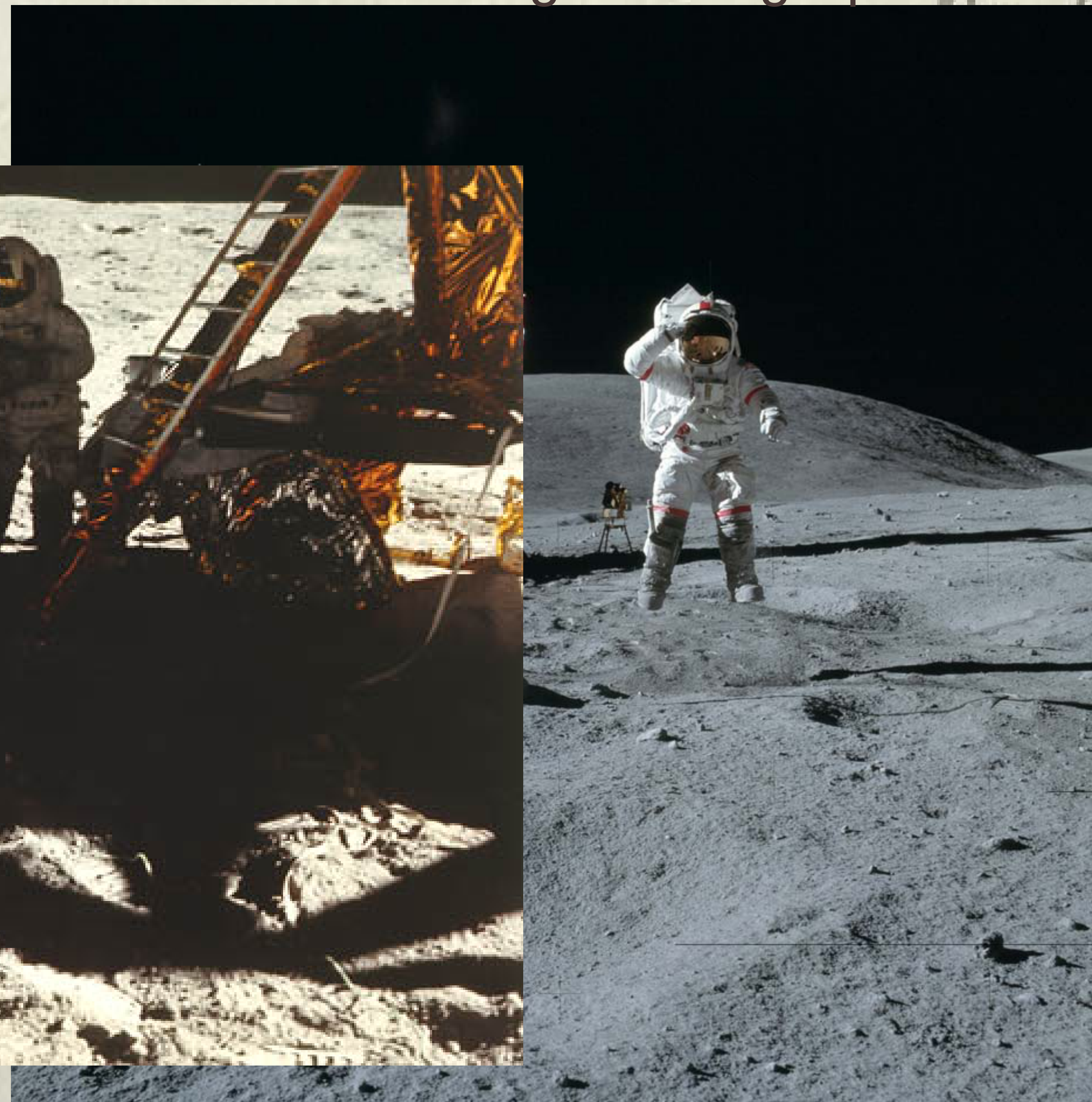

2-D imaging of Earth’s upper-atmospheric airglow emissions was first achieved with a lunar-based imager during Apollo 16.

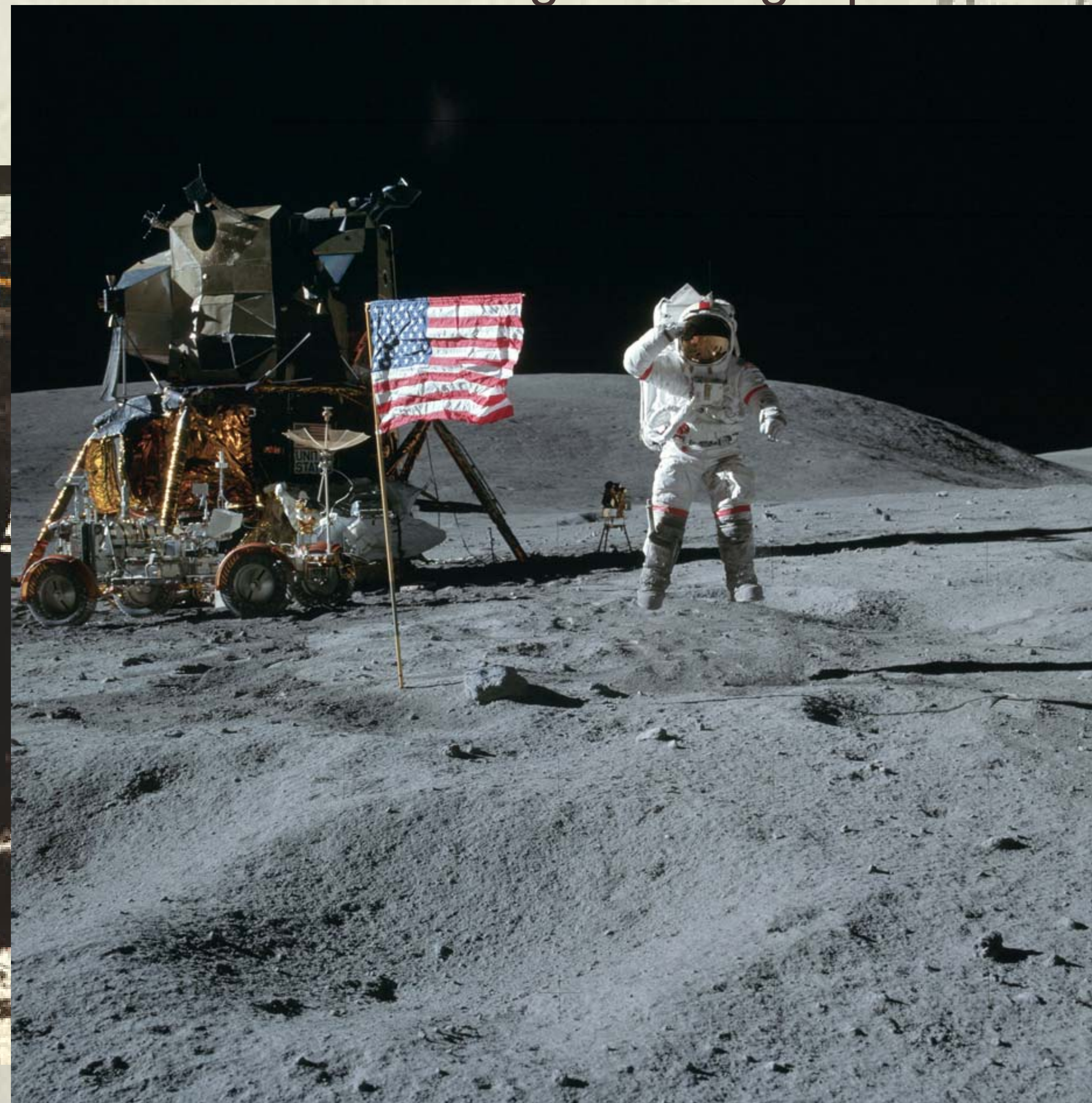

2-D imaging of Earth's airglow emissions was first achieved with a lunar-based imager during Apollo 16.

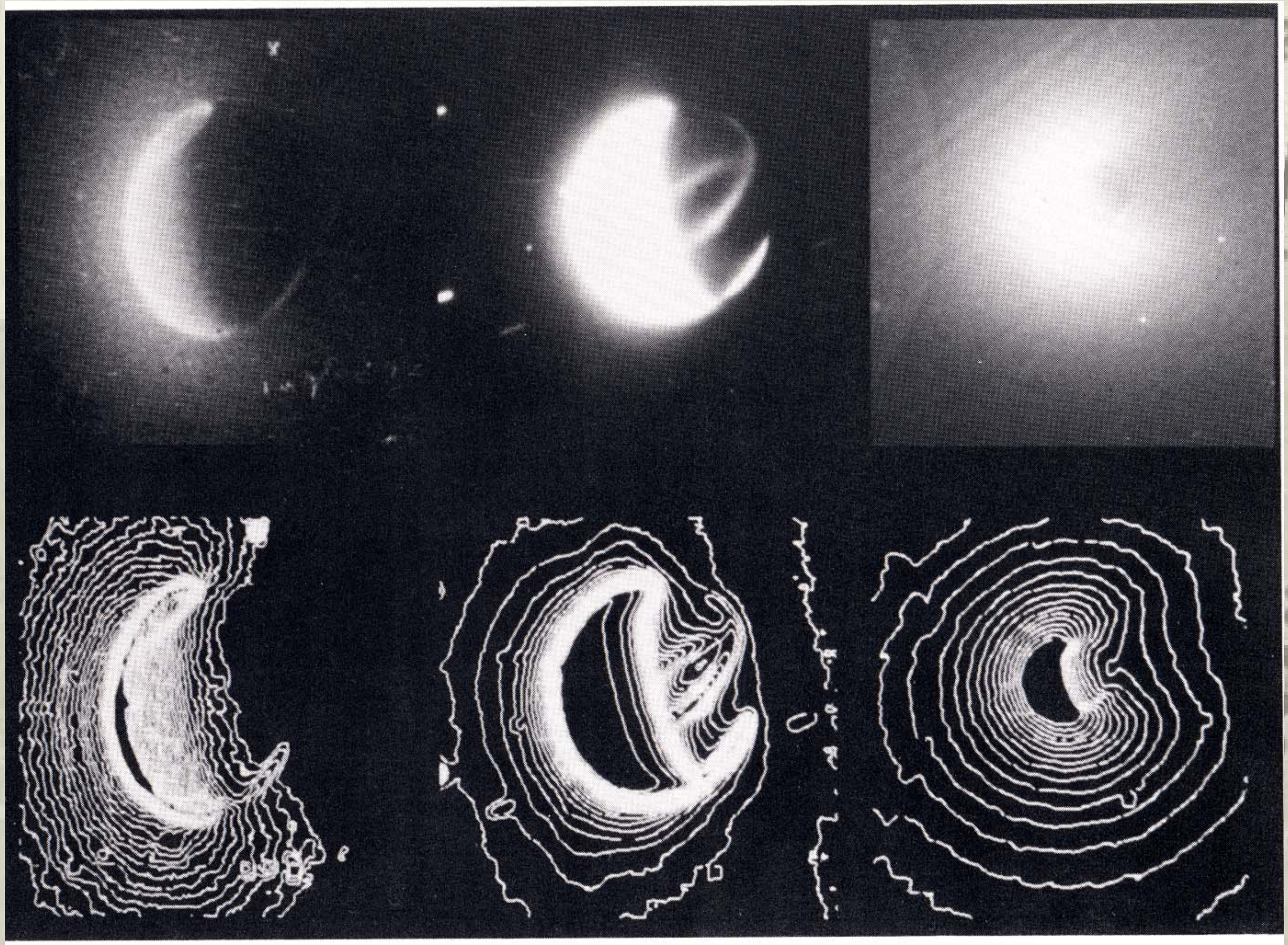

Space-based imaging

What terrestrial emissions originate in the upper atmosphere?

How might you go about measuring them to understand physical processes in the upper atmosphere?

What other experiments/datasets/models make these measurements more useful/revealing?

What have we learned from these measurements?

What do we not understand?

Space-based imaging

What terrestrial emissions originate in the upper atmosphere?

How might you go about measuring them to understand physical processes in the upper atmosphere?

What other experiments/datasets/models make these measurements more useful/revealing?

What have we learned from these measurements?

What do we not understand?

What are you going to do about it?

How do you get an Ultraviolet Earth?

Start with a star with an extended spectrum of high energy emissions

QuickTime™ and a
decompressor
are needed to see this picture.

QuickTime™ and a
decompressor
are needed to see this picture.

QuickTime™ and a
decompressor
are needed to see this picture.

How do you get an Ultraviolet Earth?

QuickTime™ and a decompressor are needed to see this picture.

Start with a star with an extended spectrum of high energy emissions

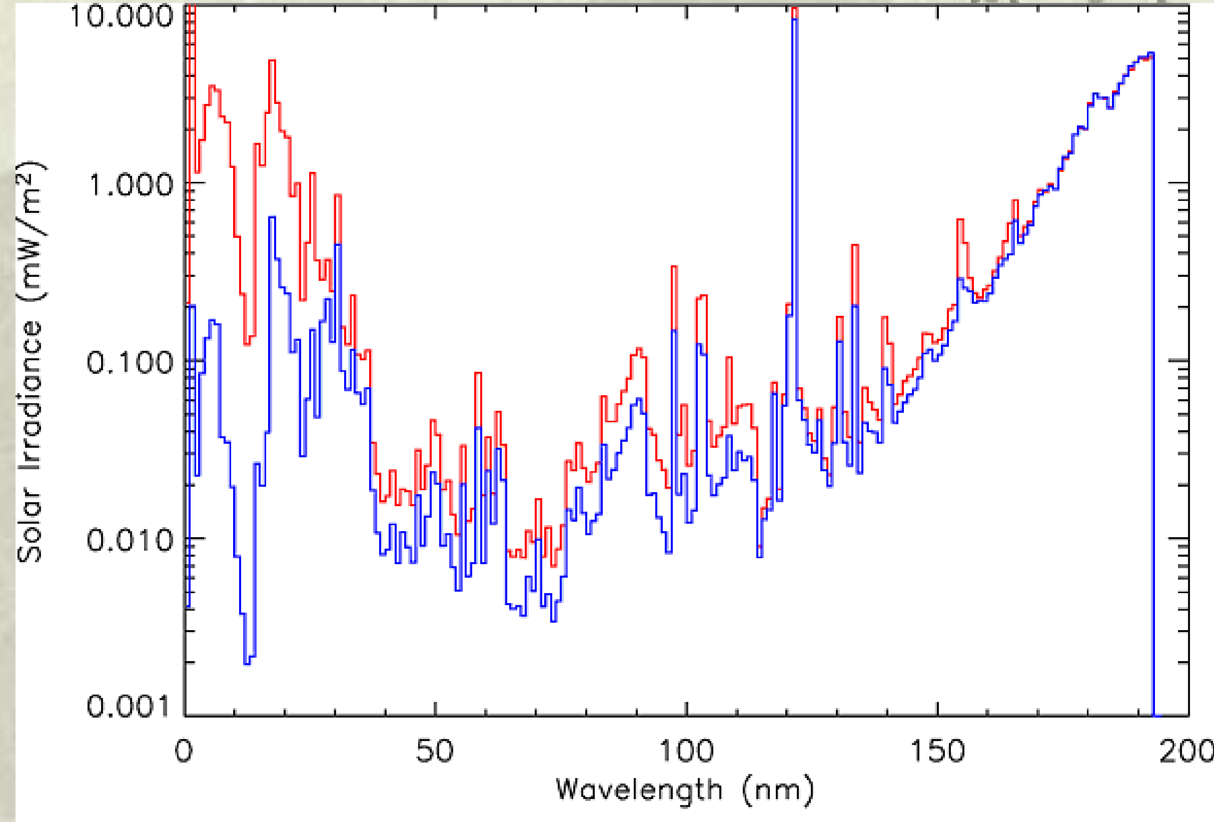

QuickTime™ and a decompressor are needed to see this picture.

Pre and post-flare EUV/FUV spectra from TIMED SEE

www.hao.ucar.edu

Ionization crossections of major species

Add a planet with N2 and O2 atmosphere. Heating and photochemistry create new important species and redistribute them with altitude.

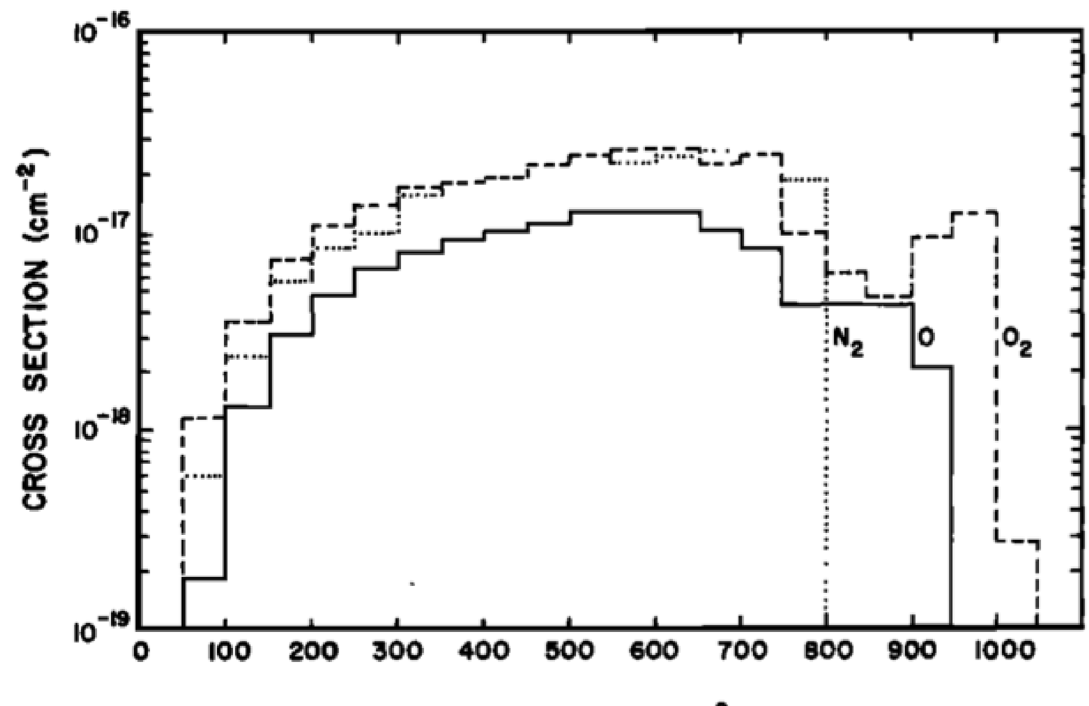

Richards and Torr (1988)

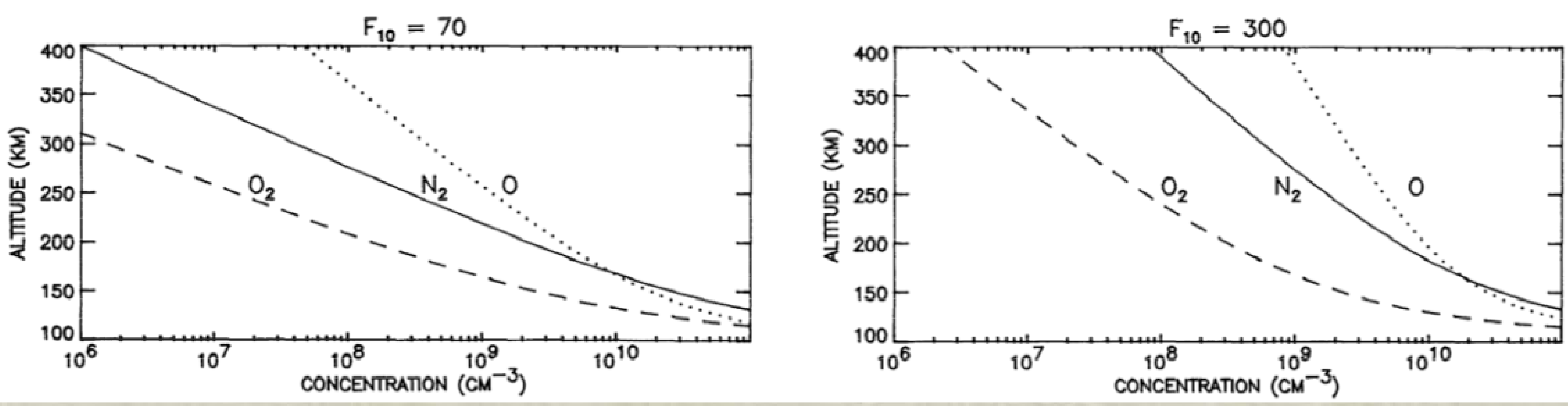

Meier and Picone (1994)

Add a planet with N2 and O2 atmosphere. Heating and photochemistry create new important species and redistribute them with altitude.

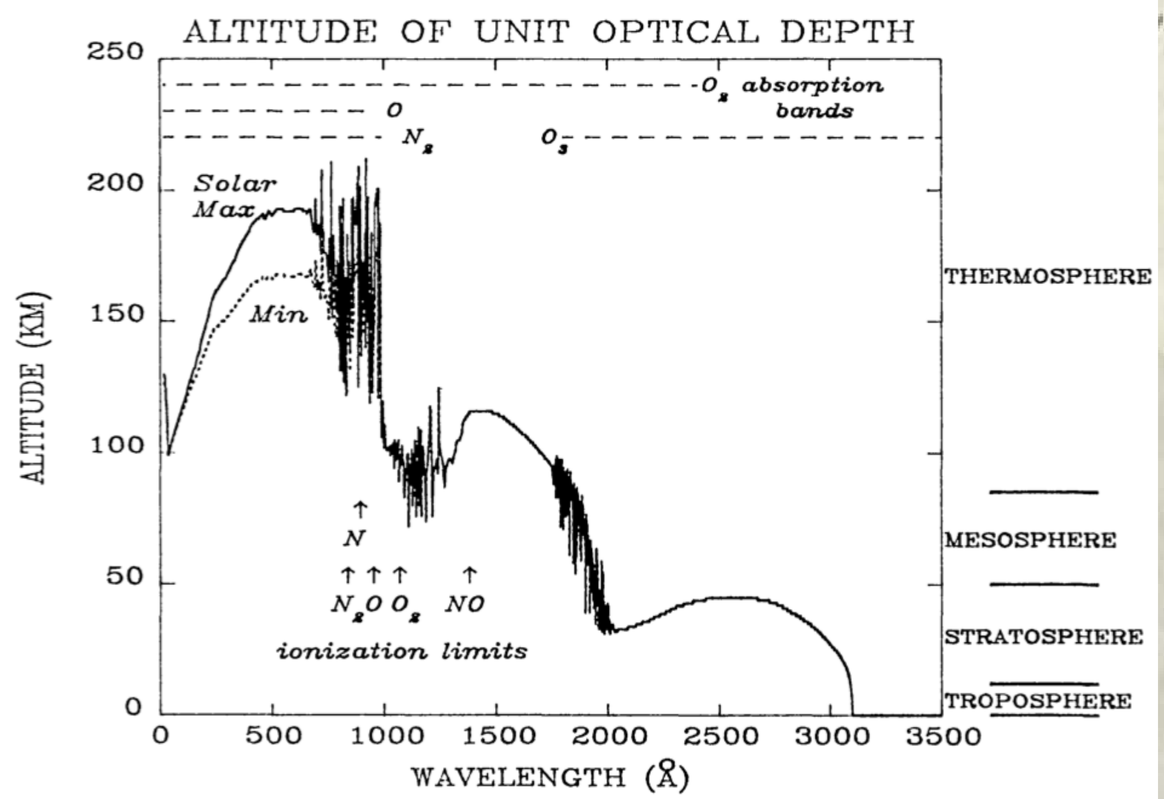

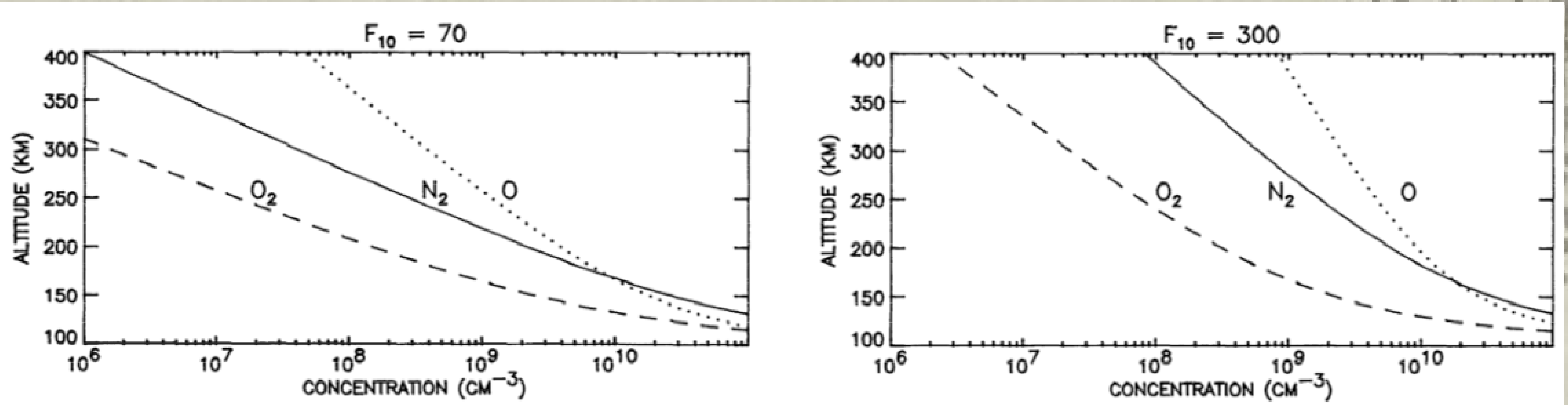

Another product of the photochemistry is a plasma, distributed in height, latitude, species, and energy.

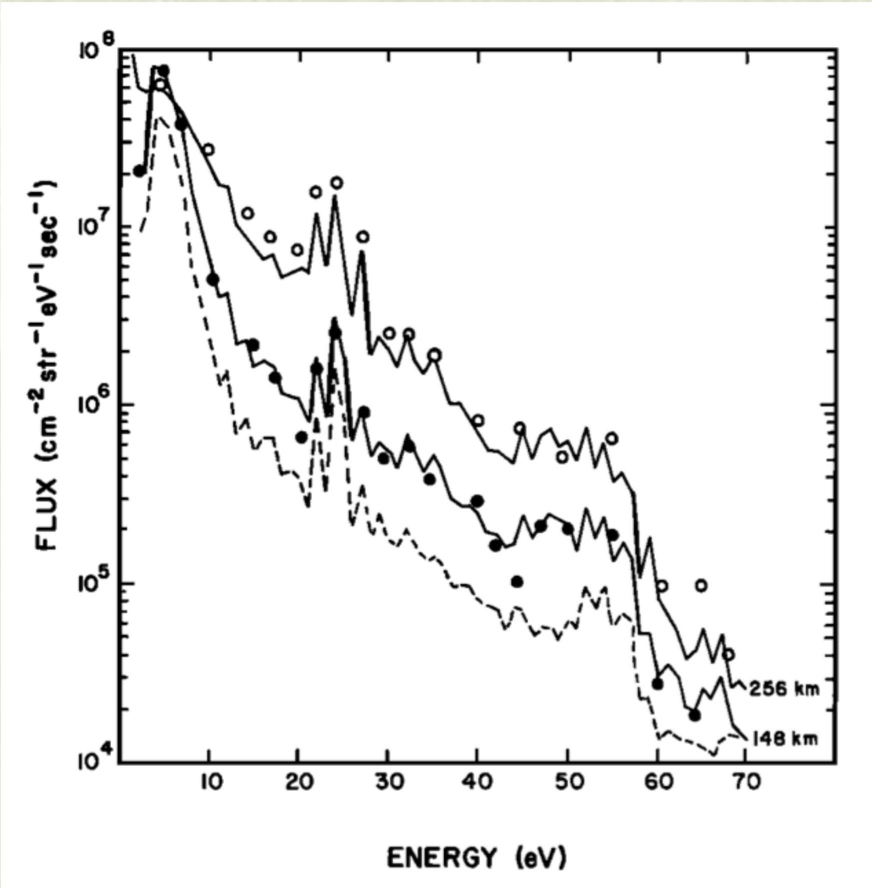

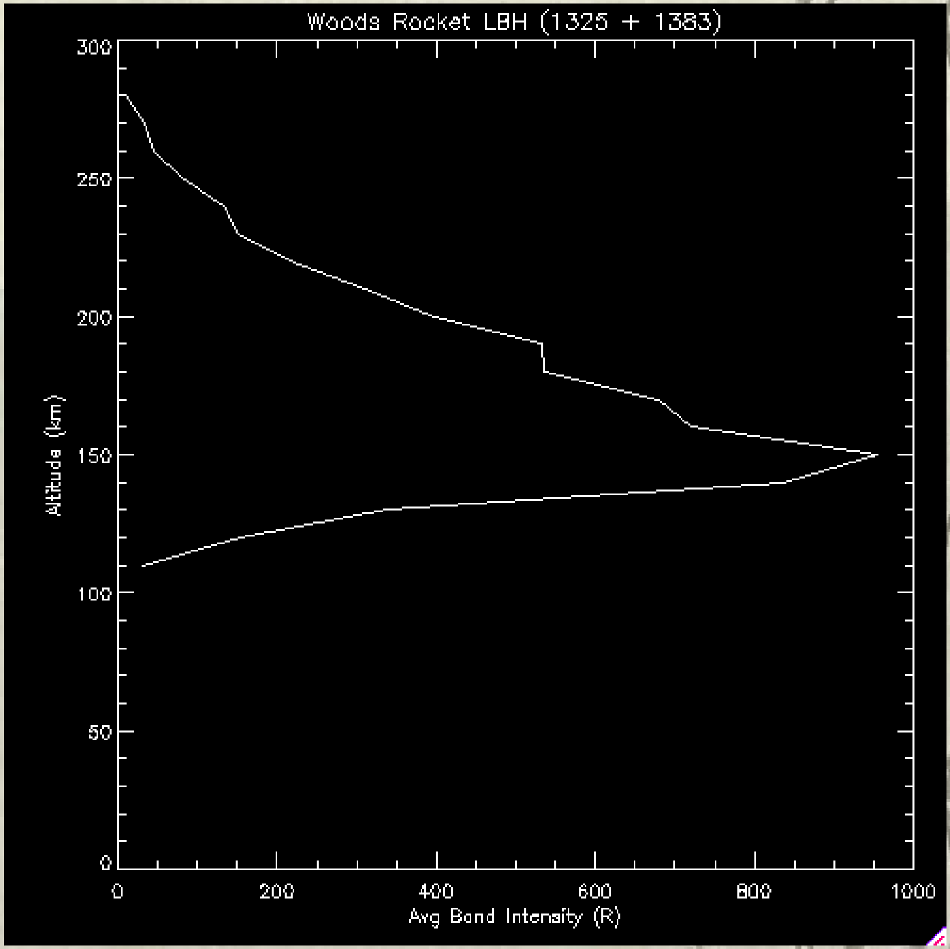

Daytime height distribution of N2 LBH emissions mirrors the altitude distribution of photoelectrons CONVOLVED with the N2 density profile.

Photoelectrons act to produce a majority of daytime FUV emissions. Earth is a net radiator at several wavelengths due to the relatively large solar EUV fluxes.

Major daytime emissions of O are at 1304 and 1356 Å. The major emission of N2 is the Lyman Birge Hopfield band system between 1350 and 2200 Å.

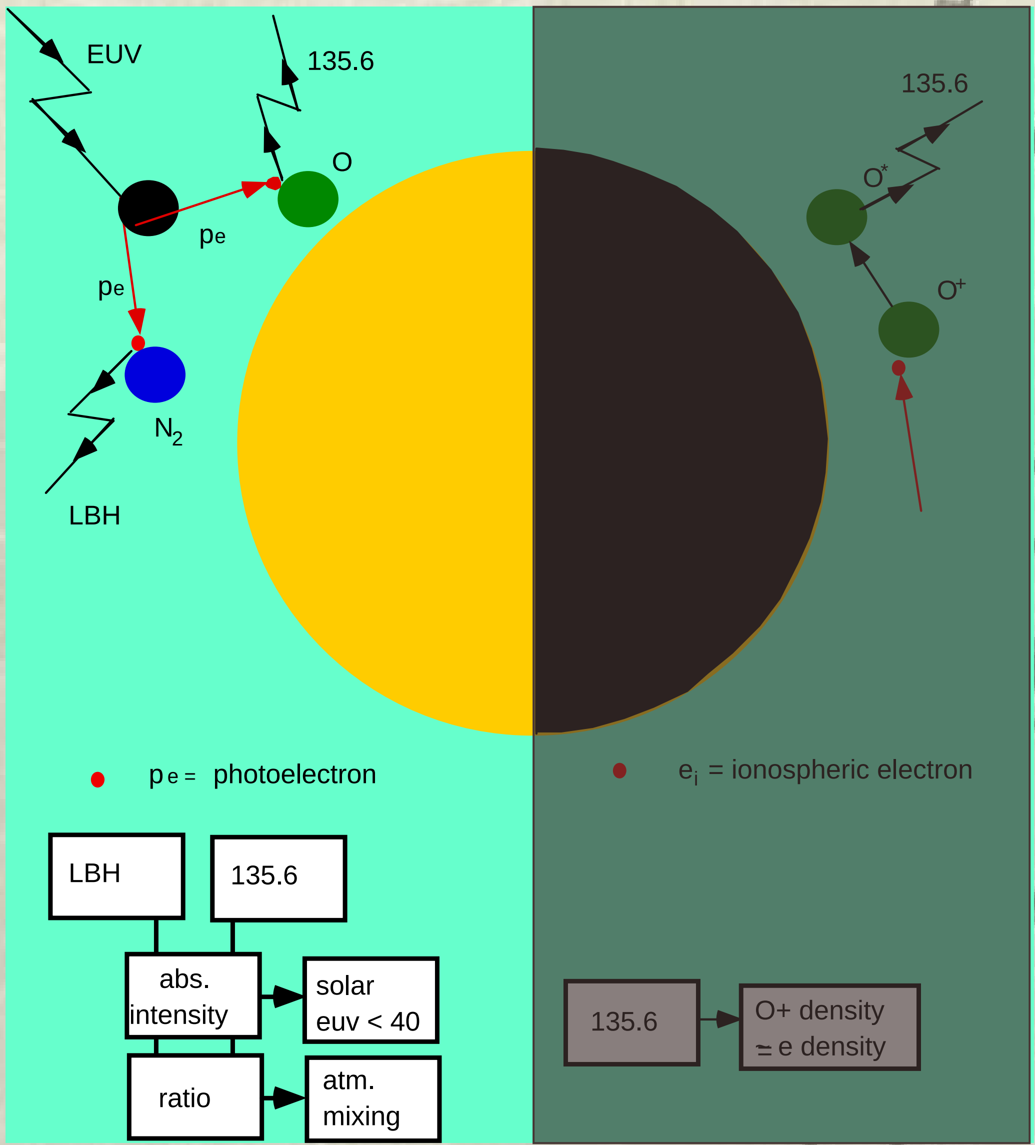

At night, photoelectron fluxes drop drastically, and recombination of ionospheric O+ is the primary source of FUV light.

Compared to daytime photoelectron-produced light, the nighttime brightness of 1356 is much more faint, though this depends greatly on latitude.

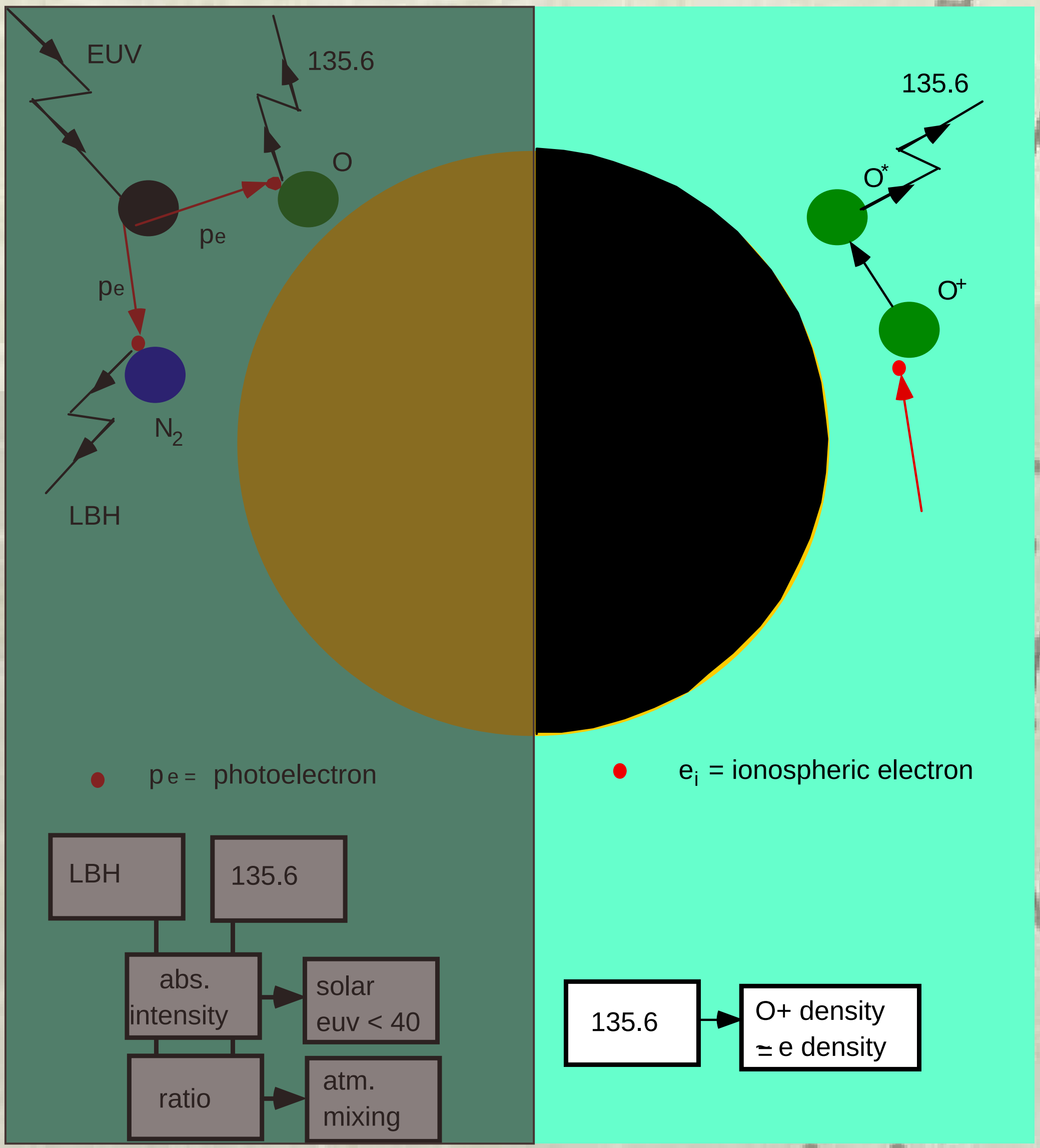

The Daytime FUV Spectrum

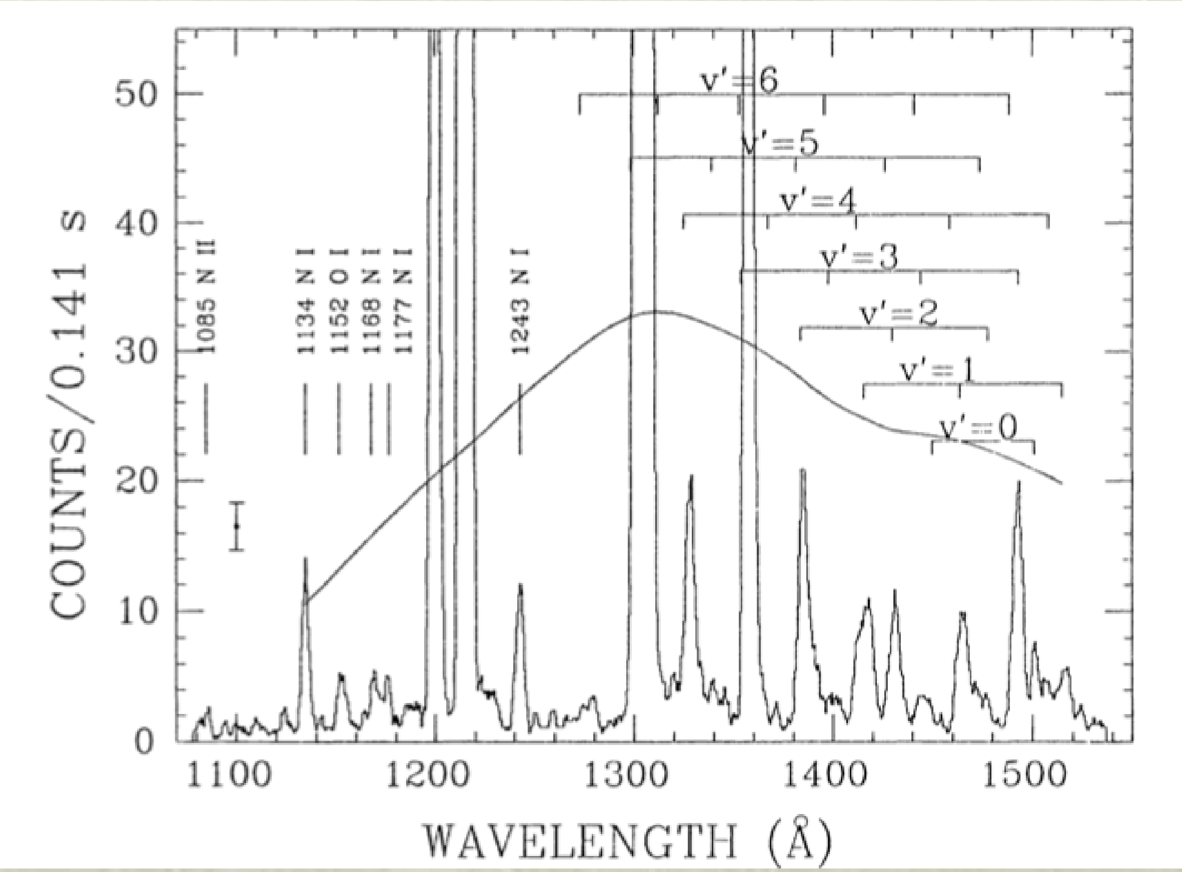

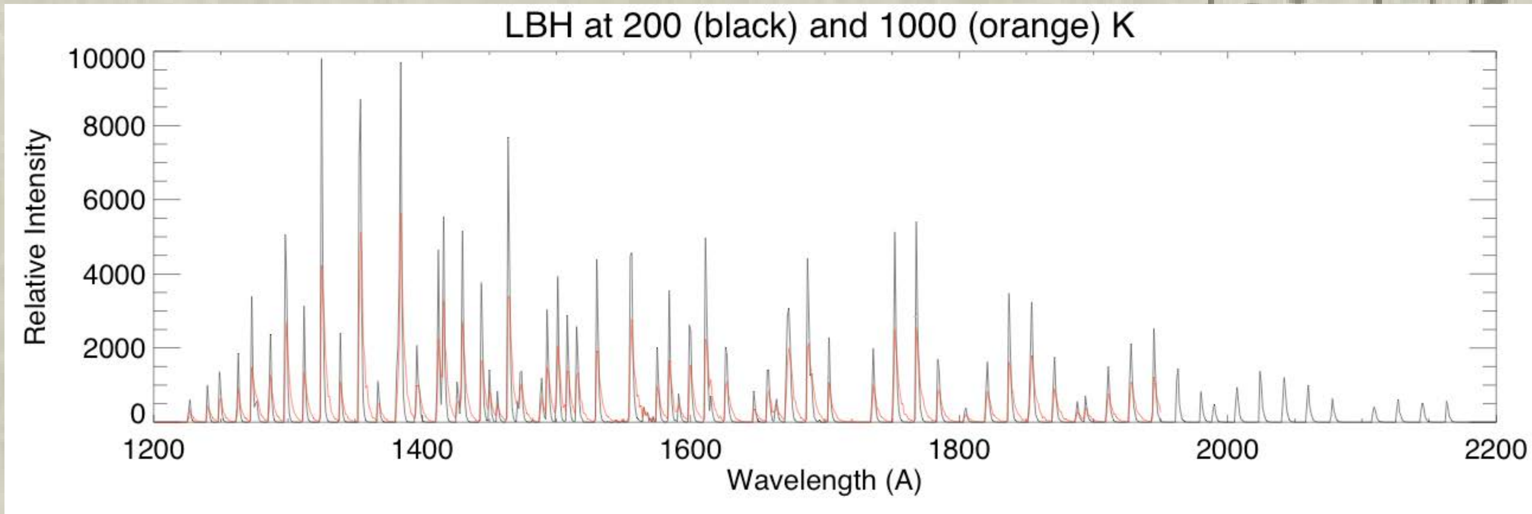

Add a fast plasma outflow from the star and a dipole field to the planet to extract energy from that magnetized plasma.

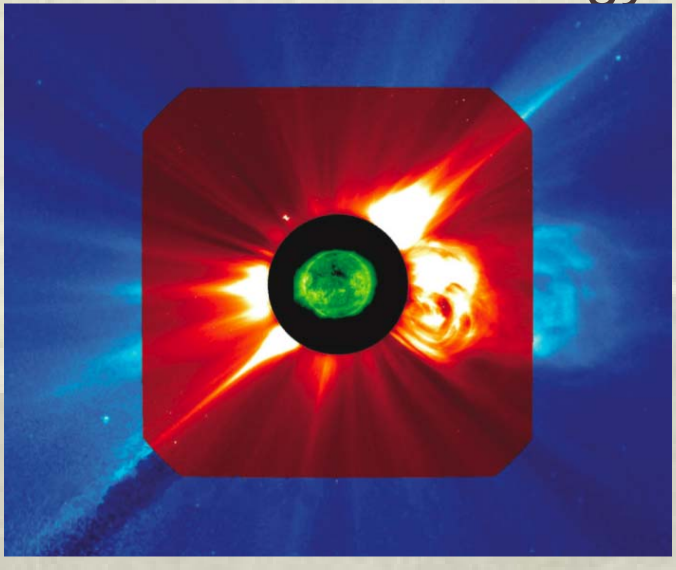

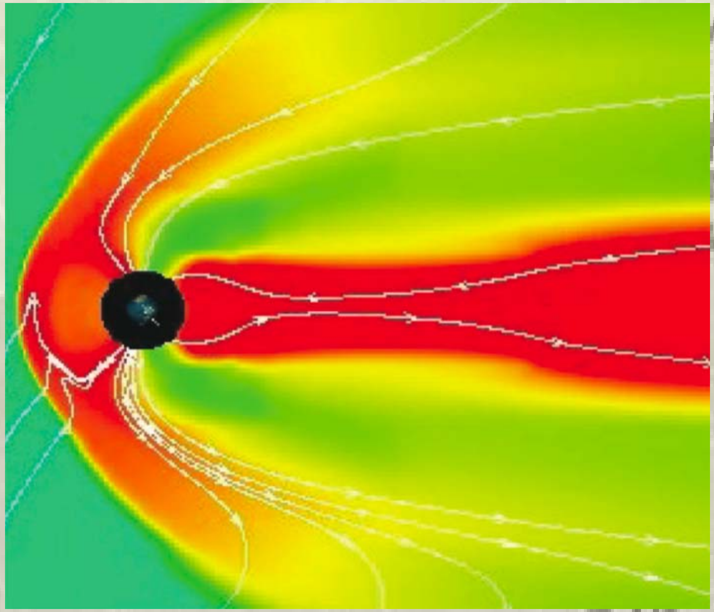

QuickTime™ and a
Cinepak decompressor
are needed to see this picture.

Coupling of magnetospheric currents, electric fields and energetic plasma distinctly modifies the atmosphere, and has a clear signature in the aurora, which is not unlike airglow in its emissions.

Retrieval of Auroral Parameters

It was apparent early on that comparisons of the ratio of particular auroral emissions in the FUV could be used to "back out" attributes such as mean energy.

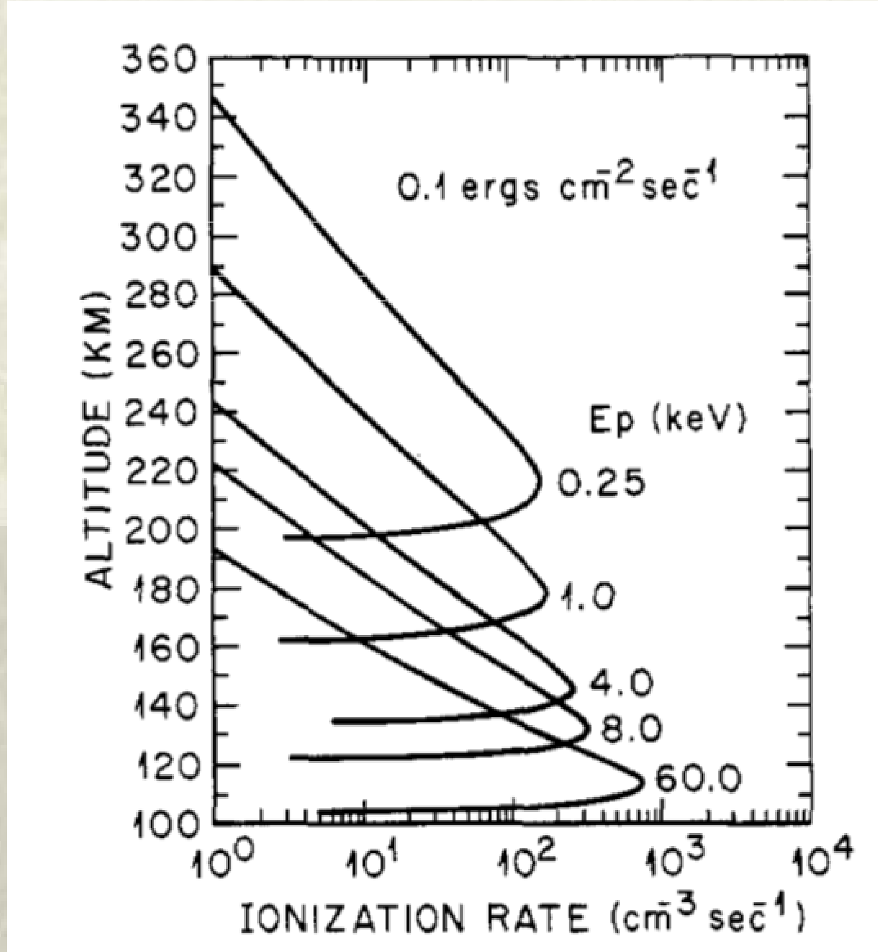

Rees (1985)

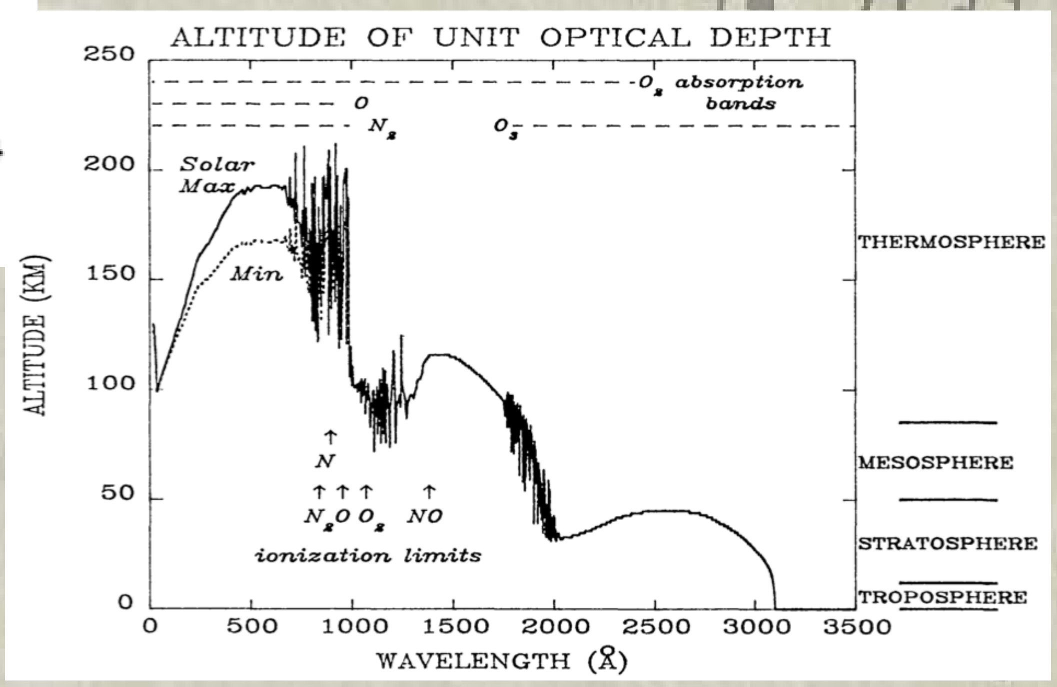

Meier (1991)

Retrieval of Auroral Parameters

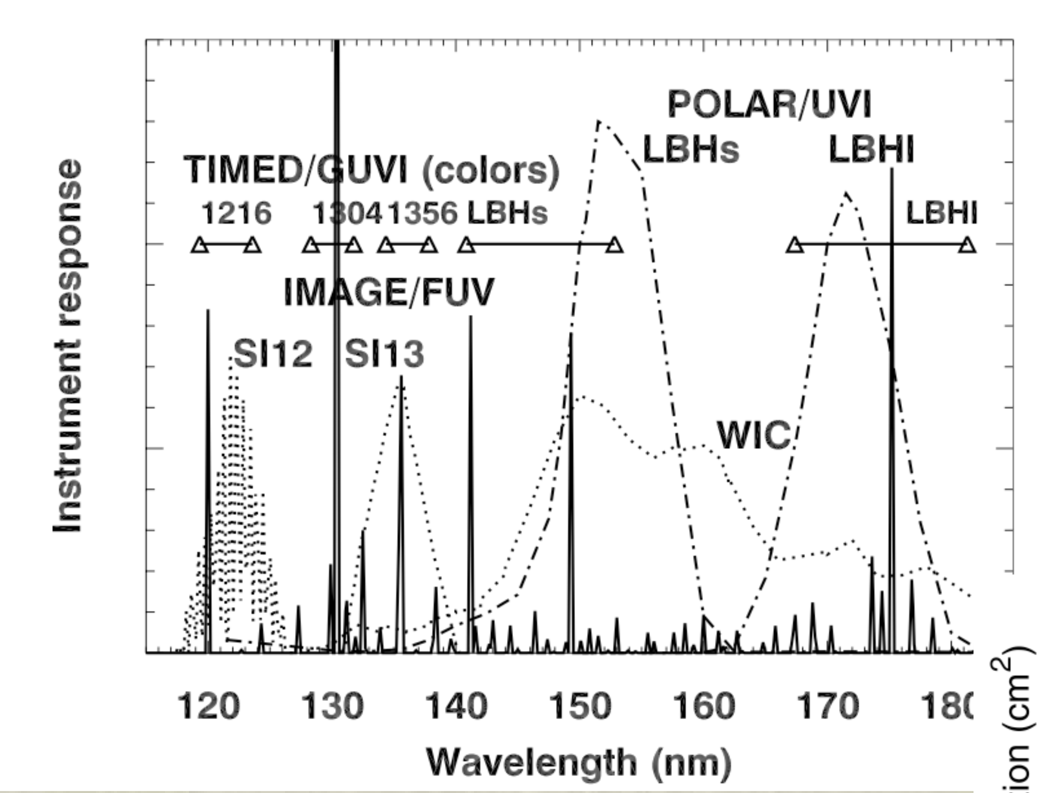

Lummerzheim and Galand (2004)

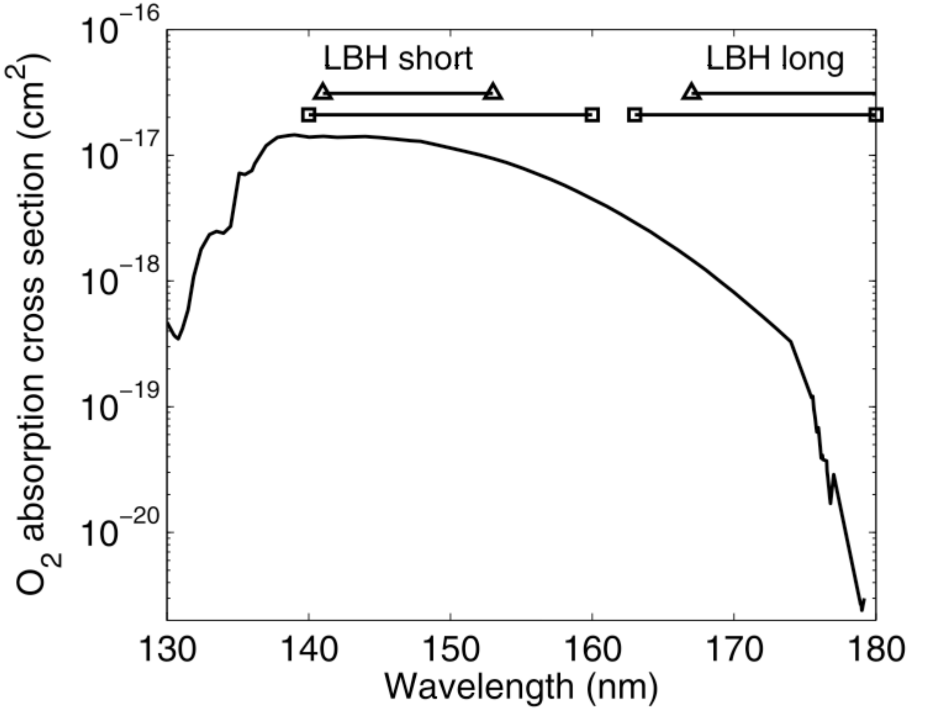

A simplified sketch of Carruther's original instrument.

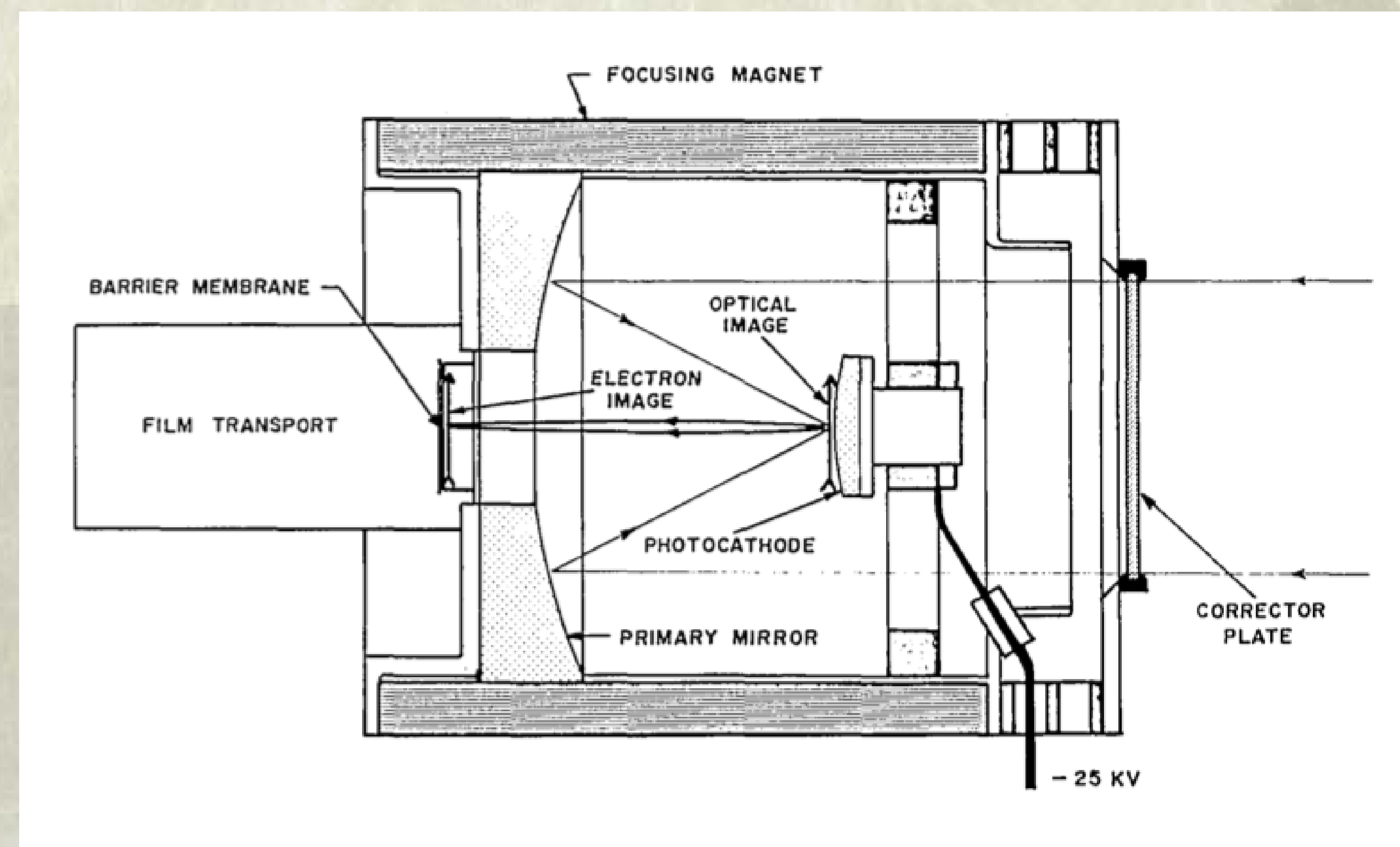

Aspects of this design continue to be used in modern UV instrumentation

Suppressive Imaging

+Large apertures

+Straightforward optical designs

-Inefficiencies of reflective optics in FUV

-Simultaneous multispectral imaging?

-Red-sensitivity can be a bear

- Dynamics Explorer SAI
- POLAR Earth Camera, UVI
- IMAGE Wideband Imaging Camera

Spectroscopic Imaging

+Simultaneous multispectral detection

+No red sensitivity

Aperature(slit) vs spectral resolution trade

- IMAGE Spectrographic Imager
- TIMED Global UV Imager
- DMSP SSUSI

Subsequent NASA missions carried instruments mainly for global-scale FUV auroral imaging.

POLAR and IMAGE

DE-1, 1981

QuickTime™ and a
decompressor
are needed to see this picture.

Polar Bear, 1986

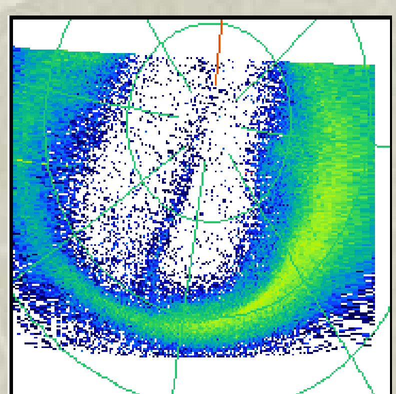

QuickTime™ and a
decompressor
are needed to see this picture.

POLAR-VIS, 1996

Subsequent NASA missions carried instruments mainly for global-scale FUV auroral imaging.

POLAR and IMAGE

DE-1, 1981

Polar Bear, 1986

QuickTime™ and a
decompressor
are needed to see this picture.

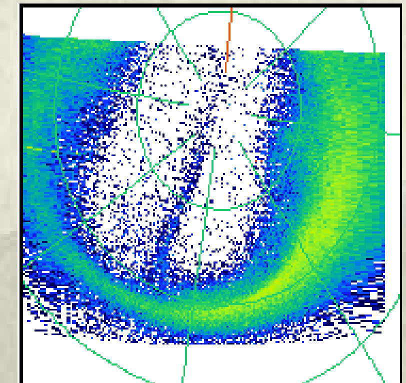

QuickTime™ and a
decompressor
are needed to see this picture.

POLAR-VIS, 1996

1304 and 1356 OI images were repurposed for I-T imaging.

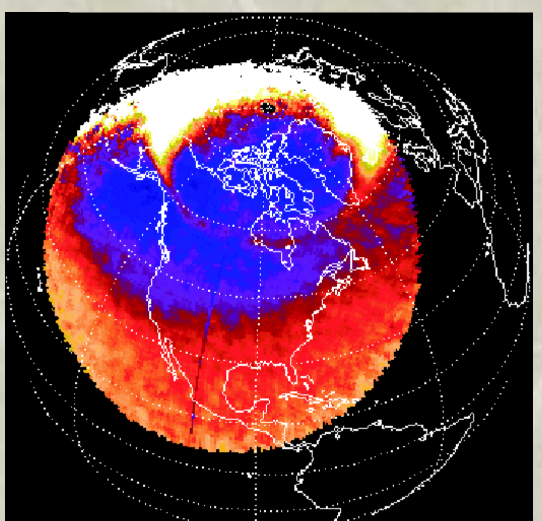

DE-1

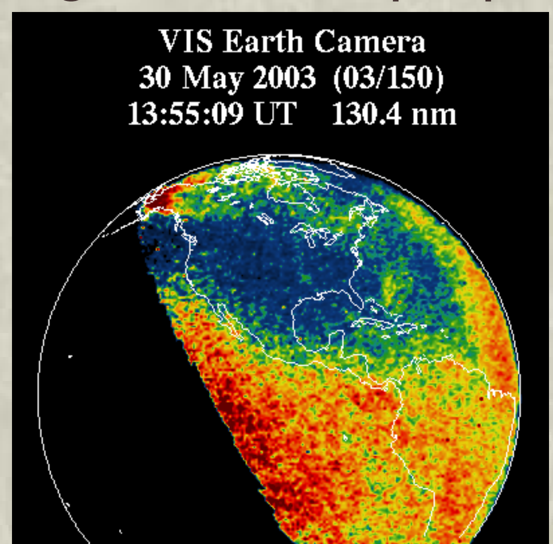

POLAR-VIS

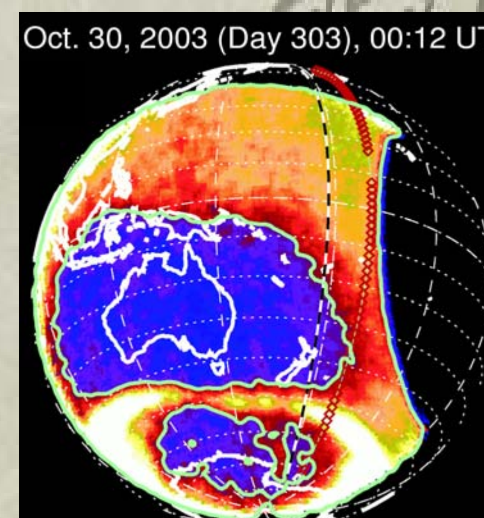

IMAGE

The Thermospheric Storm

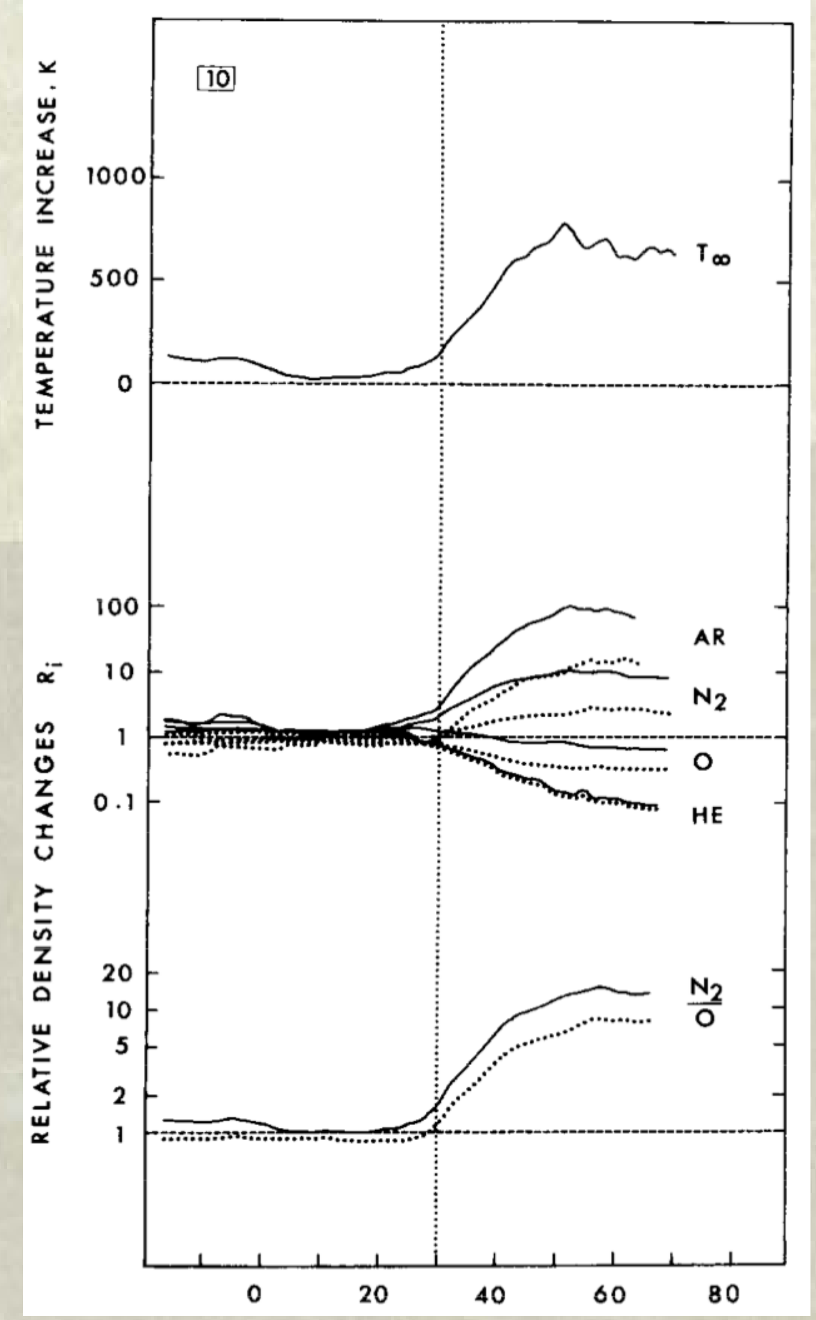

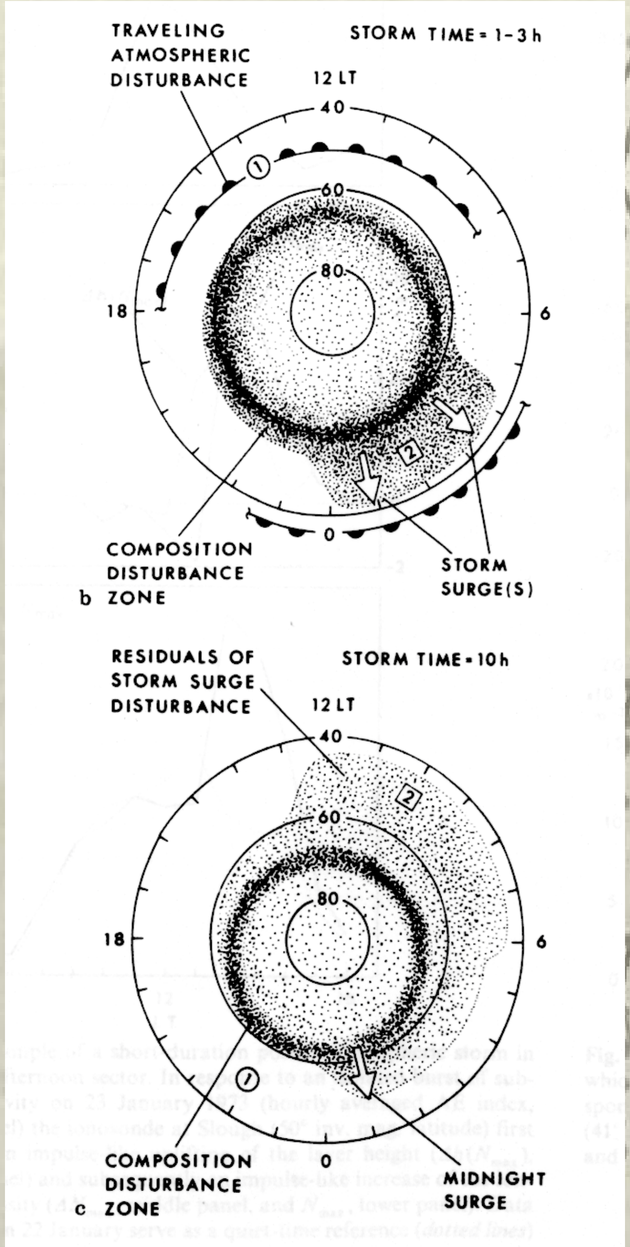

Pr□ölss (1987)

Composition effects driven by storm-time thermospheric winds at storm onset.

Positive and Negative Phases

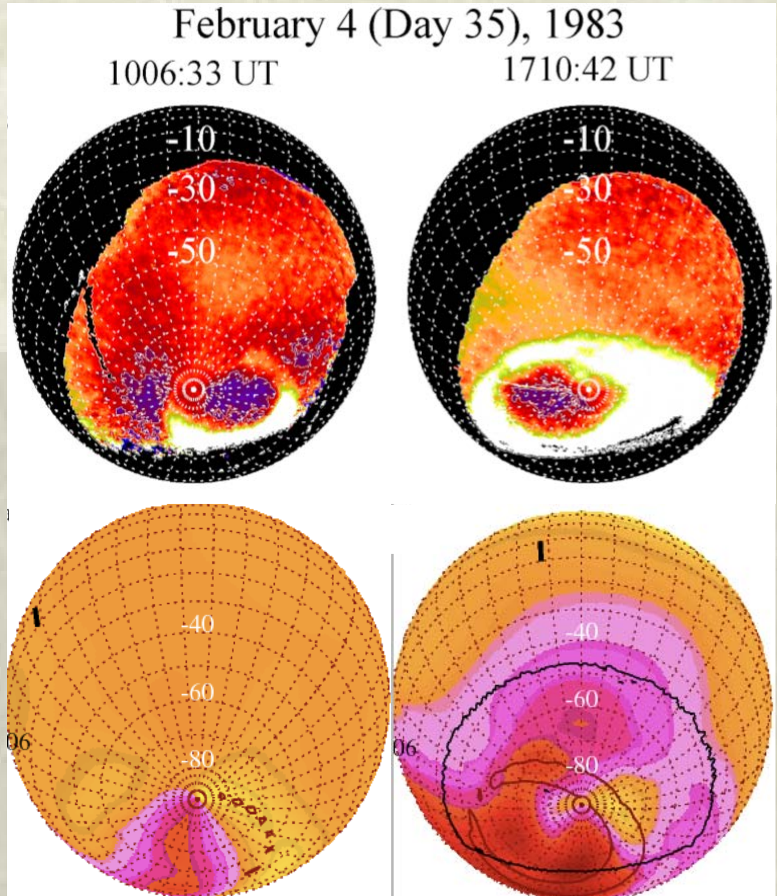

Immel et al 2001

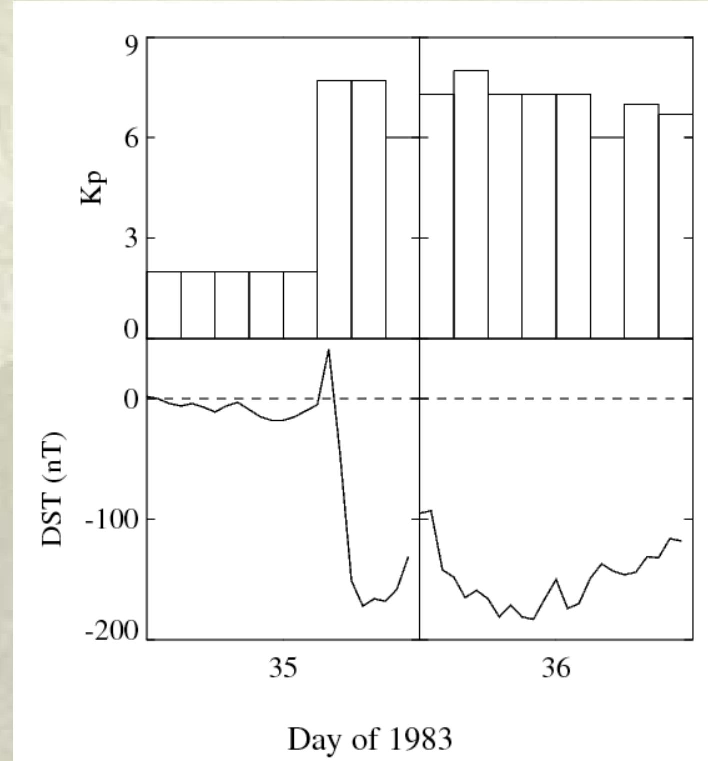

Composition effects driven by high-latitude Joule during the storm.

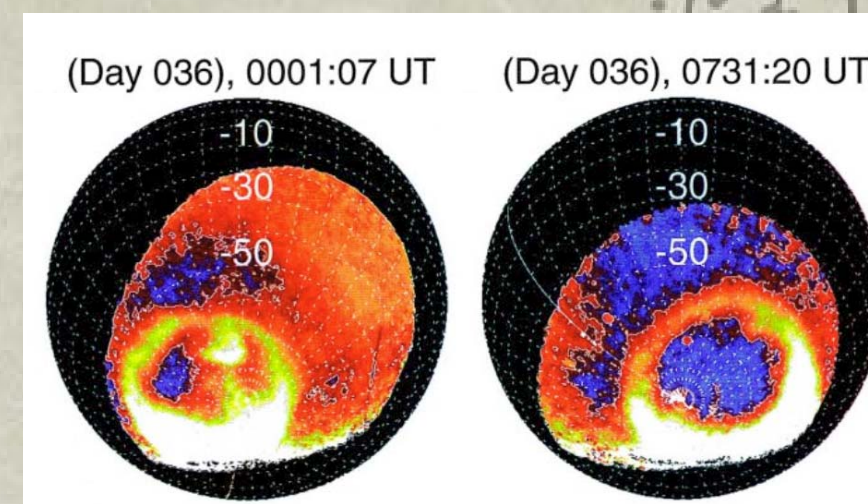

Ionospheric F-peak density effects driven by changes in composition.

The Ionospheric Storm

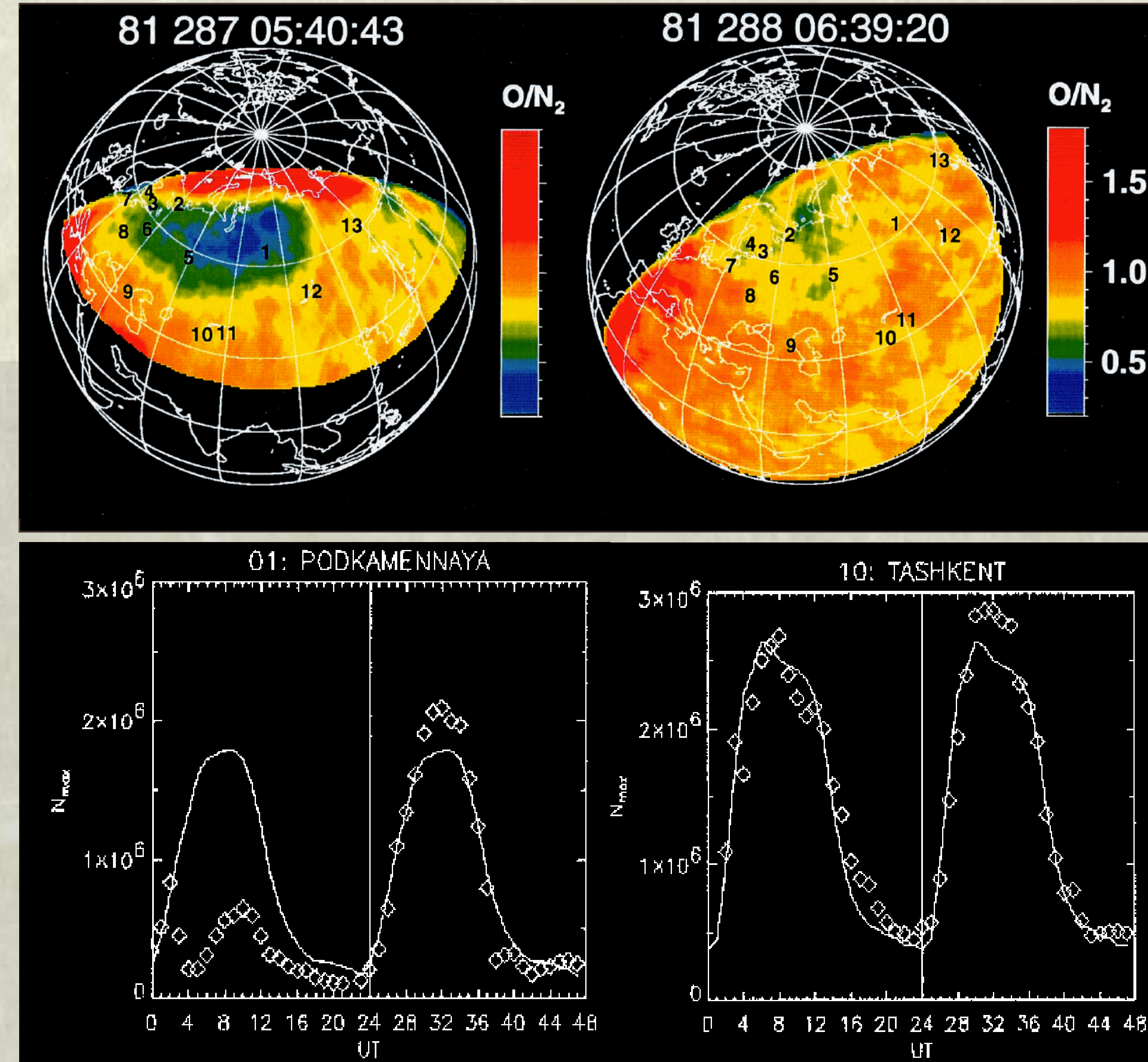

Strickland et al. (2005)

An Open Question: Competing Effects

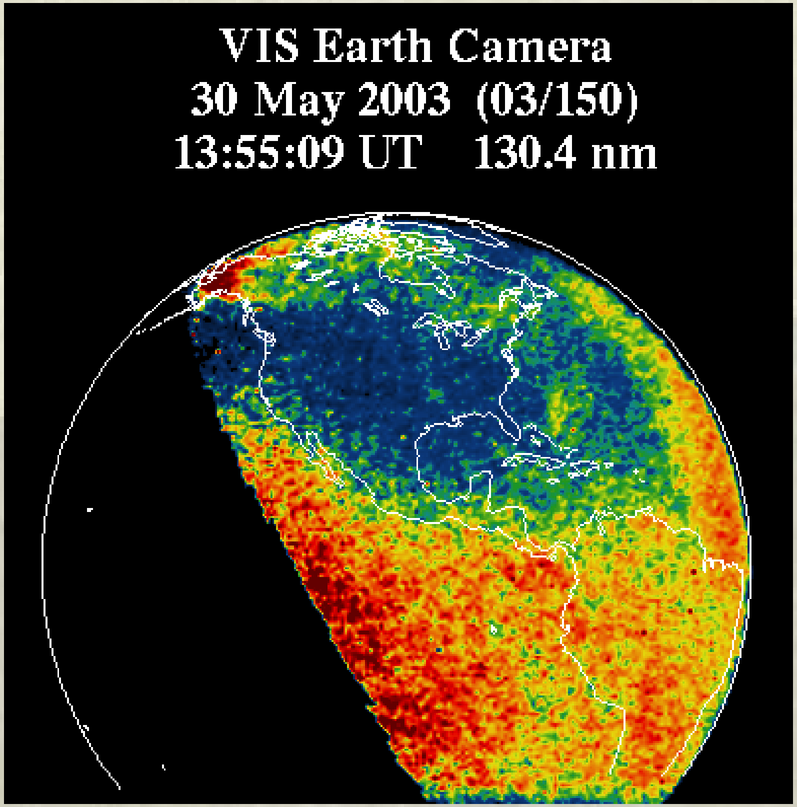

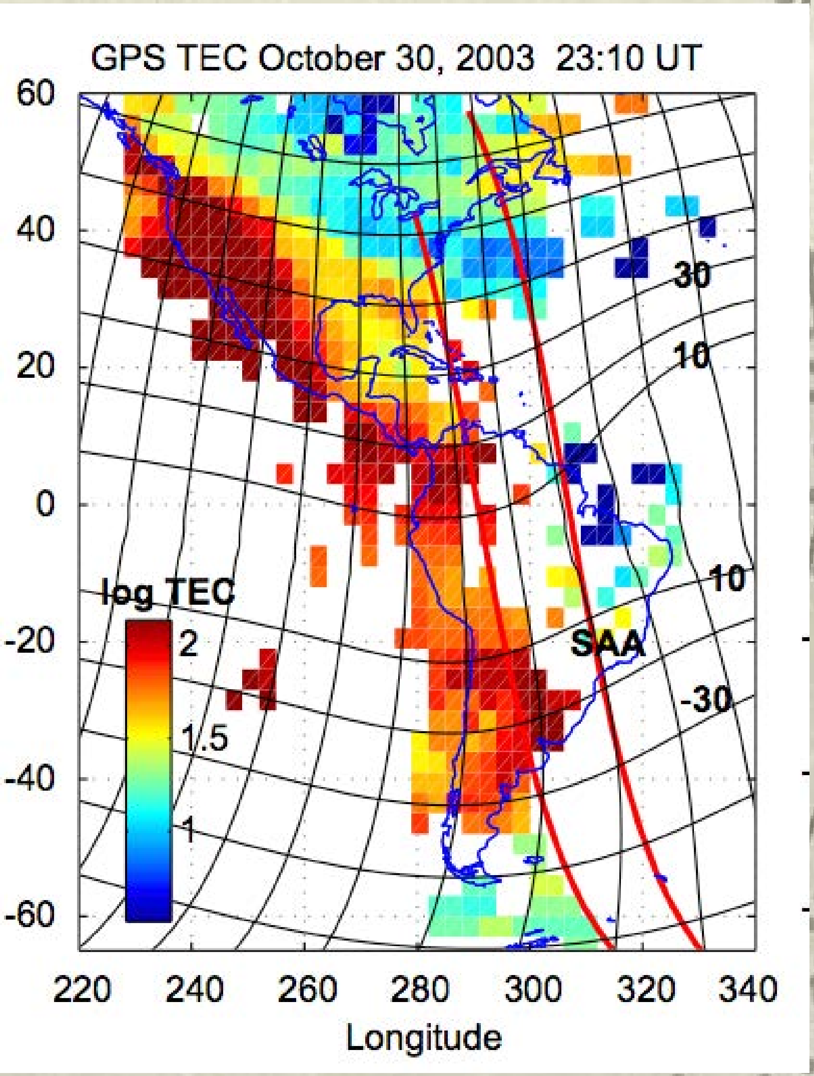

Composition disturbances vs. storm-enhanced density. Who wins?

Foster and Coster (2007)

From the daytime FUV airglow, disk imaging reveals global effects on O/N2, but with imaging of OI emissions, is more or less limited to column integrated O/N2 retrieval.

Limb imaging, where the altitude profile of emission brightness is determined, can give new insights into many upper atmospheric phenomena.

One orbit (night-day-night) of GUVI limb data (low mag activity)

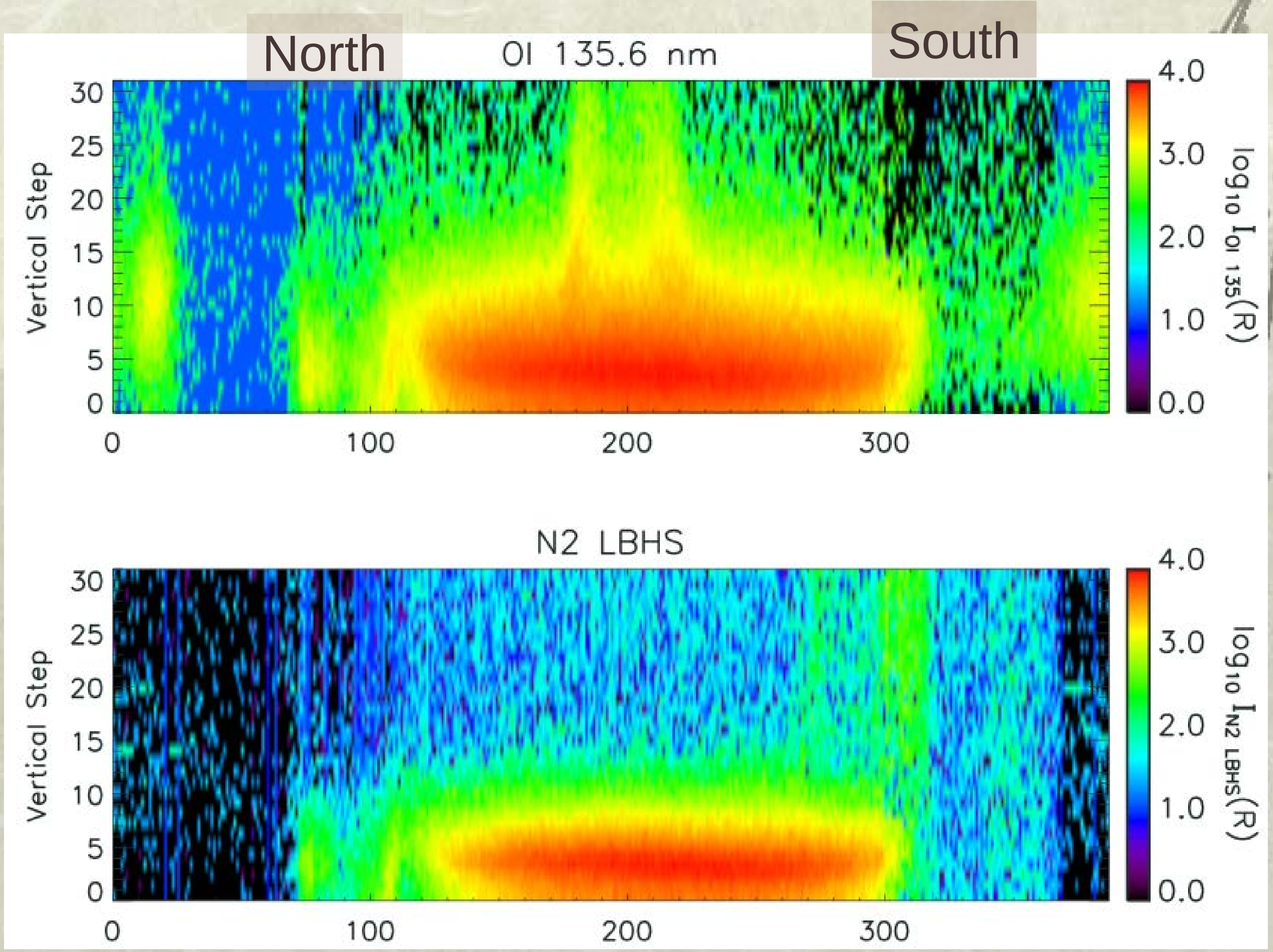

Meier et al., (2005)

135.6 and LBH-short

One orbit (night-day-night) of GUVI limb data (Nov. 2003 Storm)

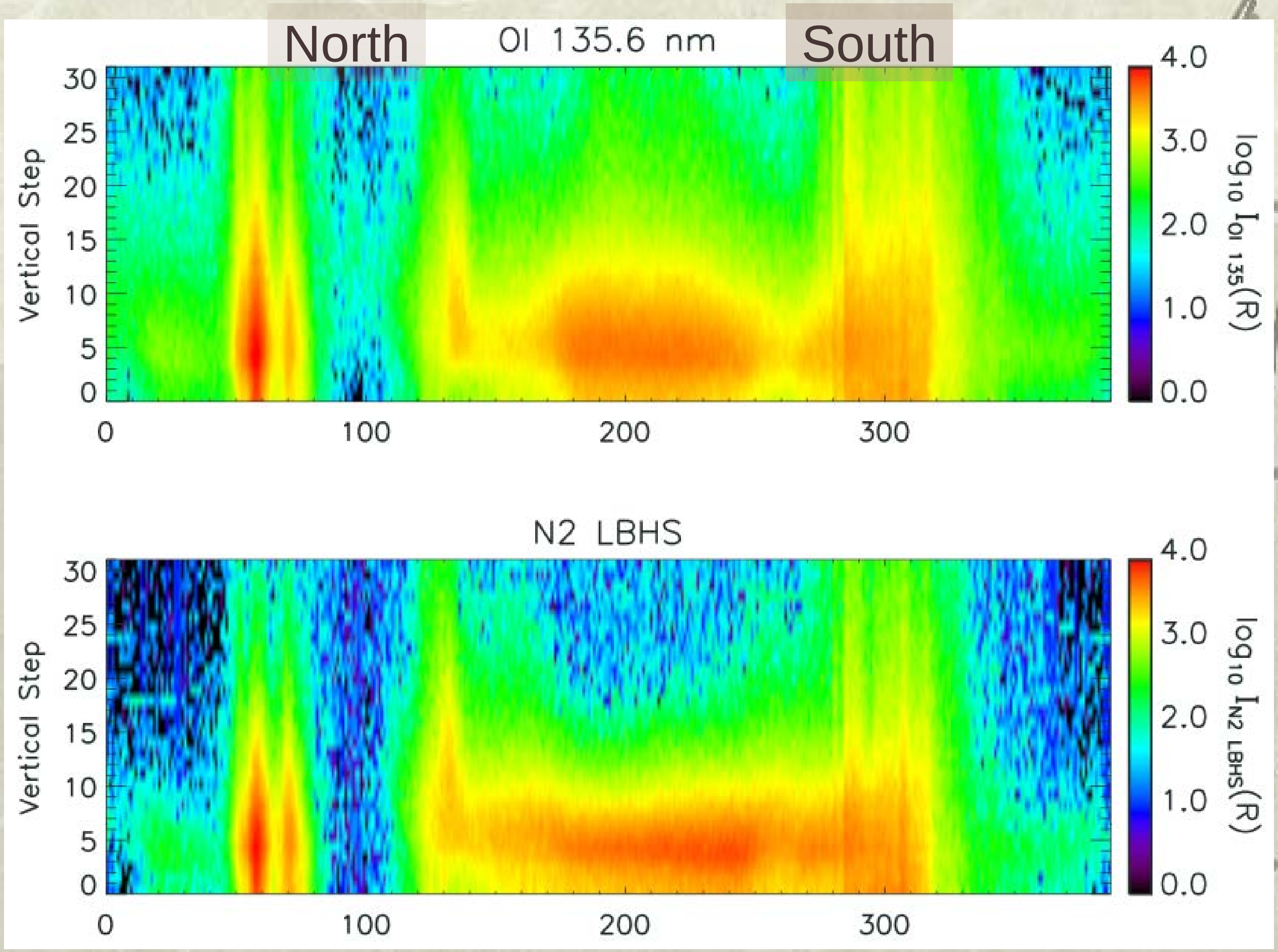

Meier et al., (2005)

135.6 and LBH-short

Using discrete inverse numerical techniques, neutral composition, temperature, and total density can be retrieved in from the daytime limb.

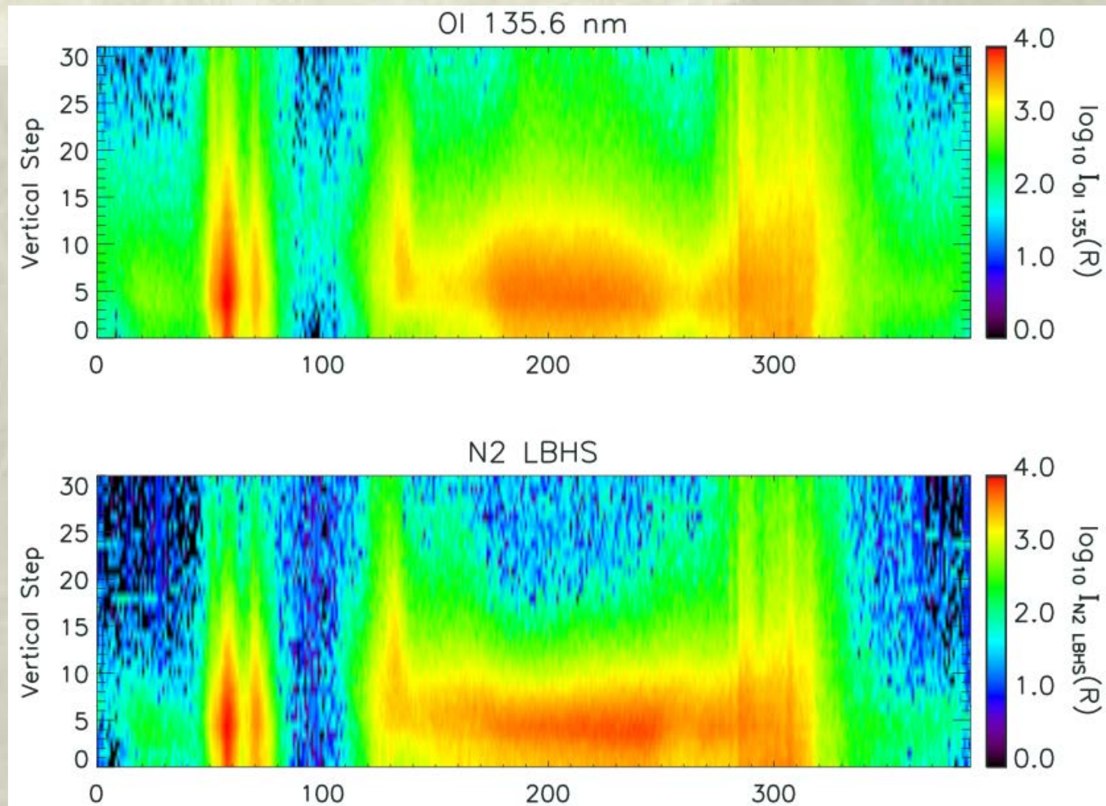

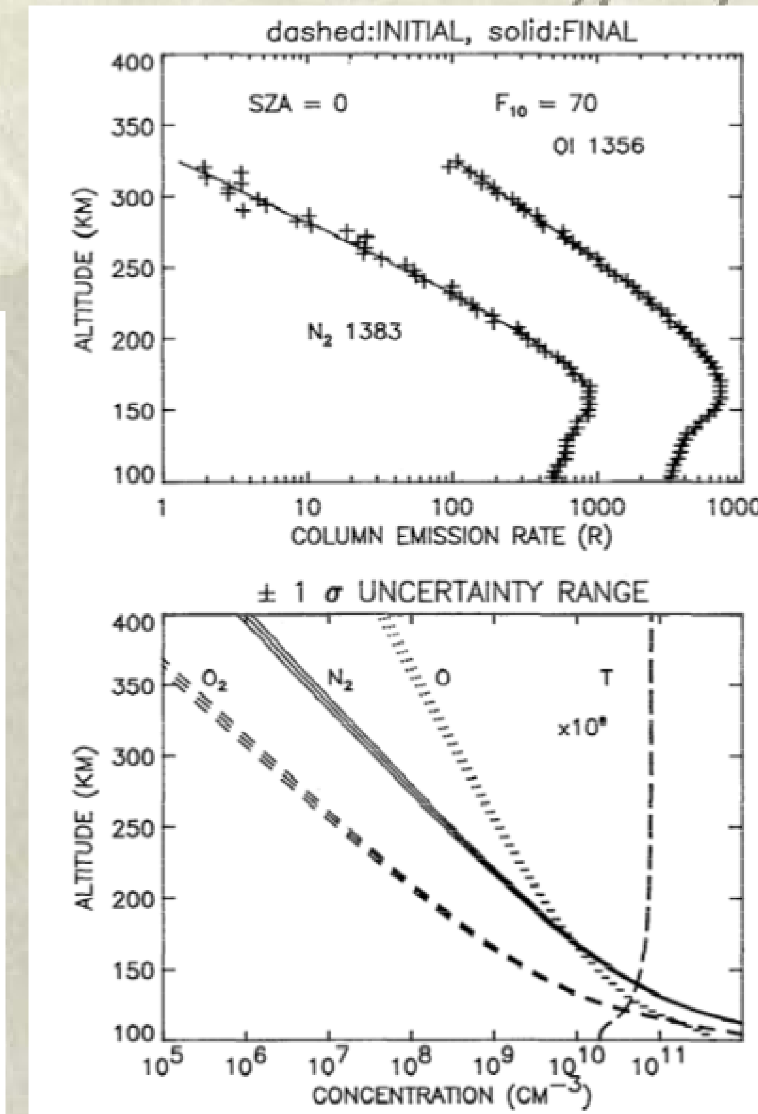

GUVI does disk imaging at fixed slowly varying local time (here, 1330 h). The occurrence of the Nov 2003 magnetic storm is again manifested in O/N2 ratios.

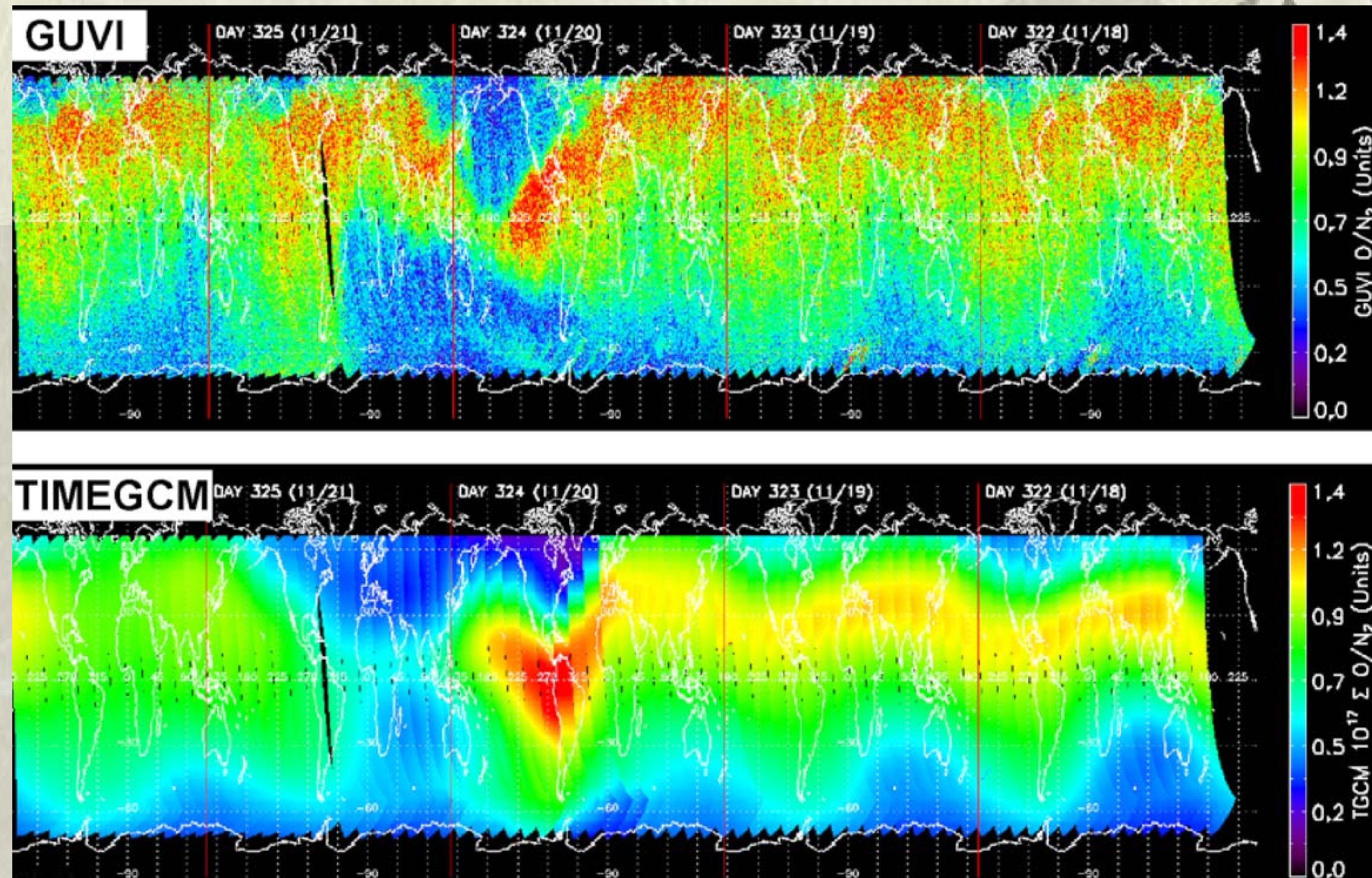

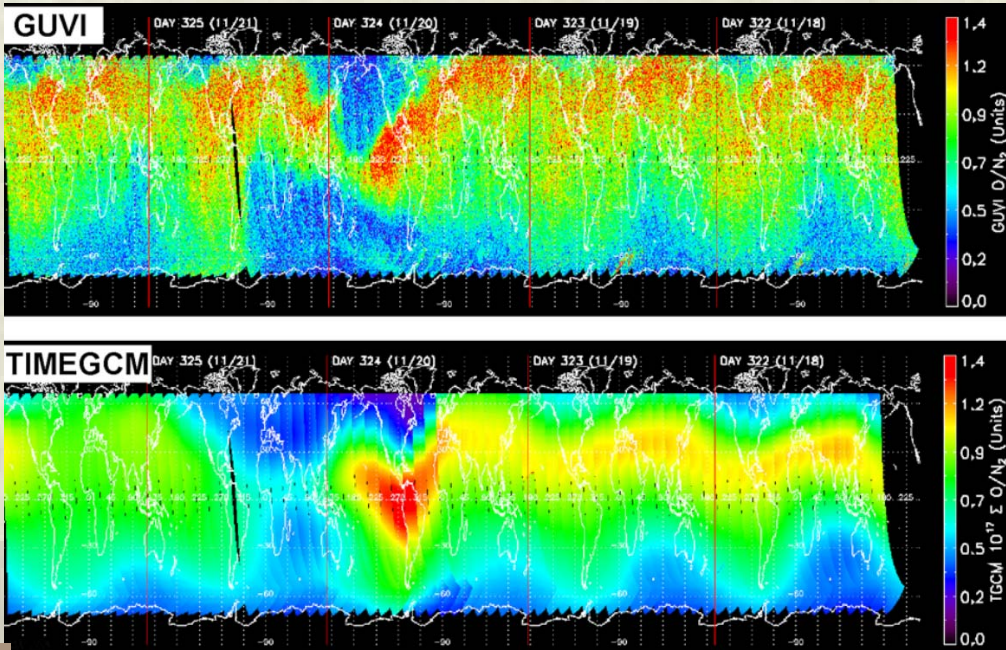

GUVI **disk** imaging yields O/N2 ratios

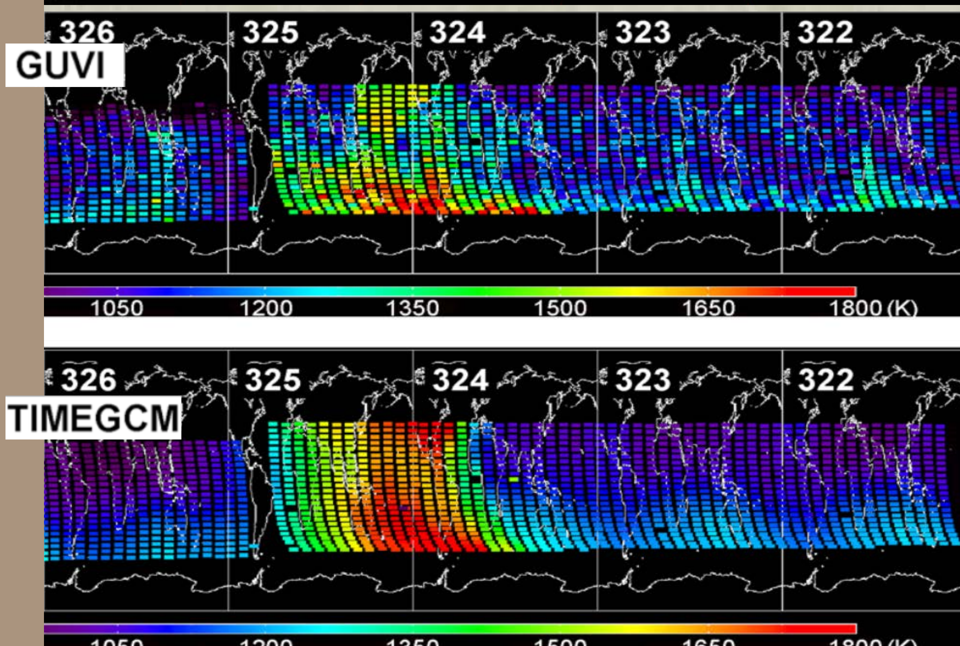

GUVI **limb** imaging allows simultaneous retrieval of exospheric temperatures

Meier et al. (2005)

Combining imaging and in-situ observations.

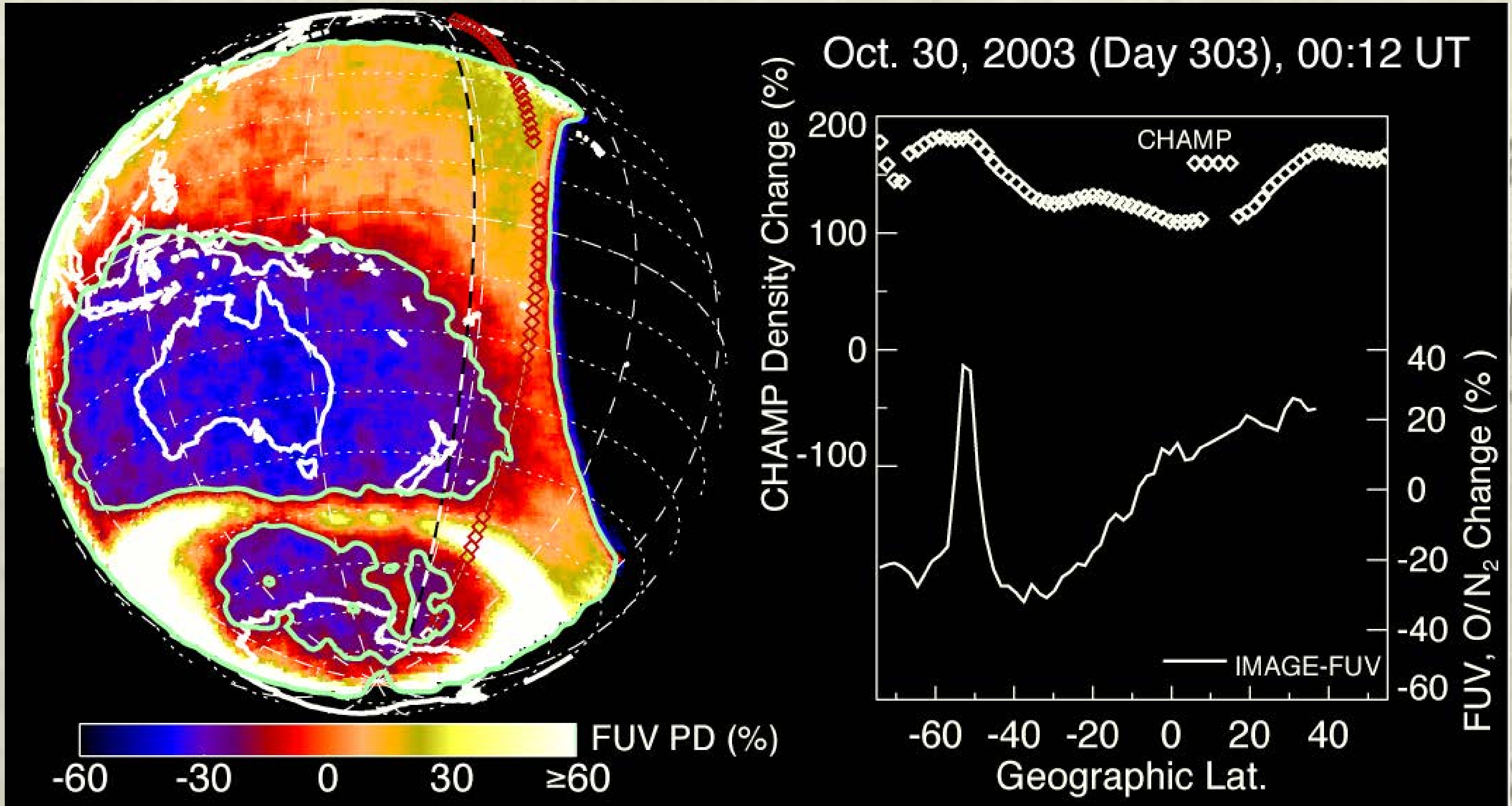

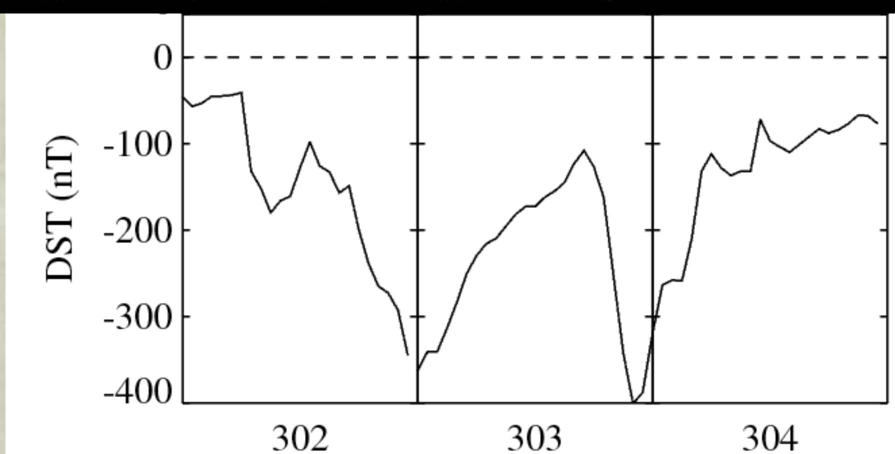

CHAMP reports density enhancements during the Oct 2003 superstorm while IMAGE-SI-13 estimates the O/N2 reduction in the morning sector.

Combining imaging and in-situ observations.

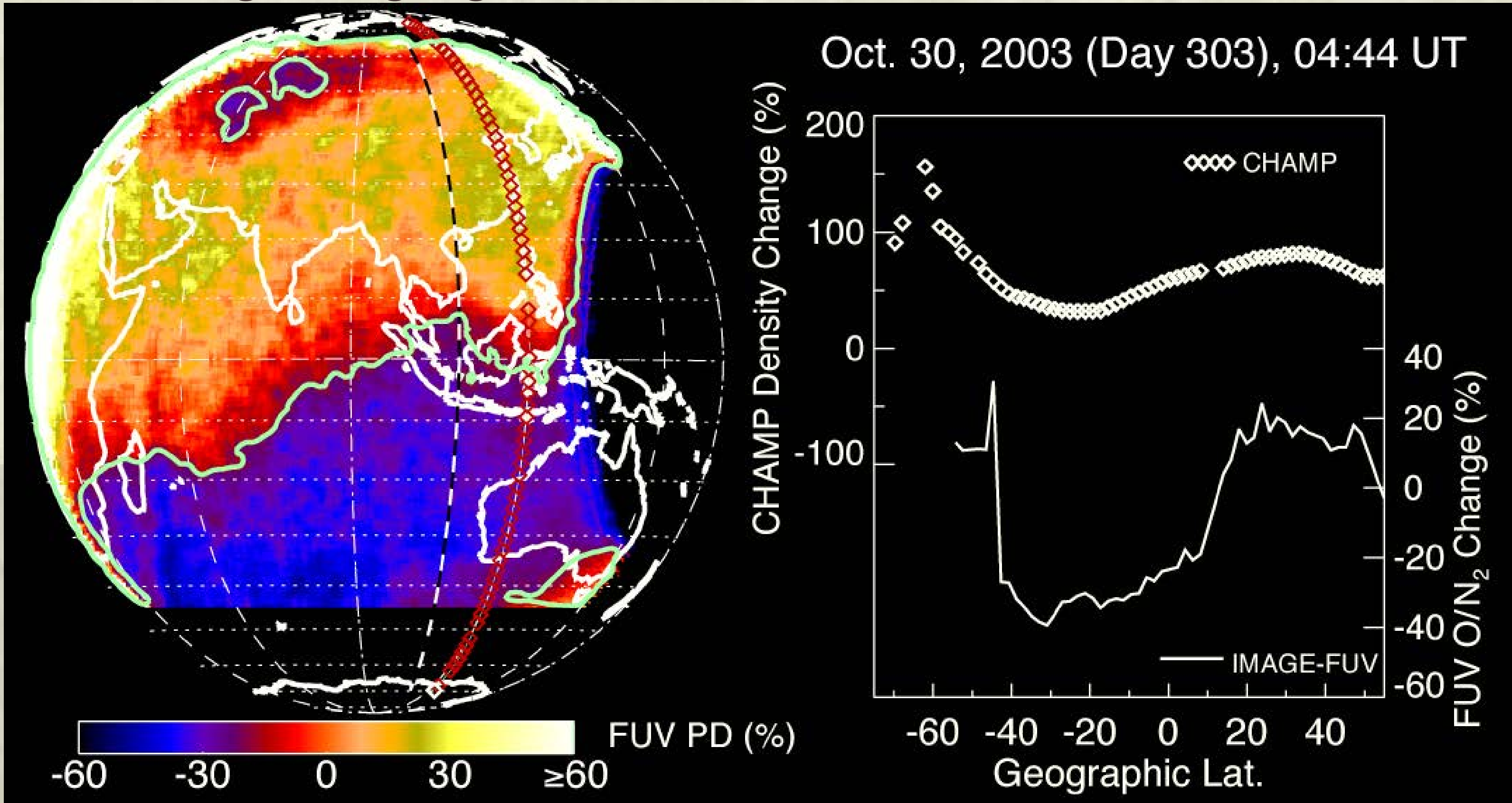

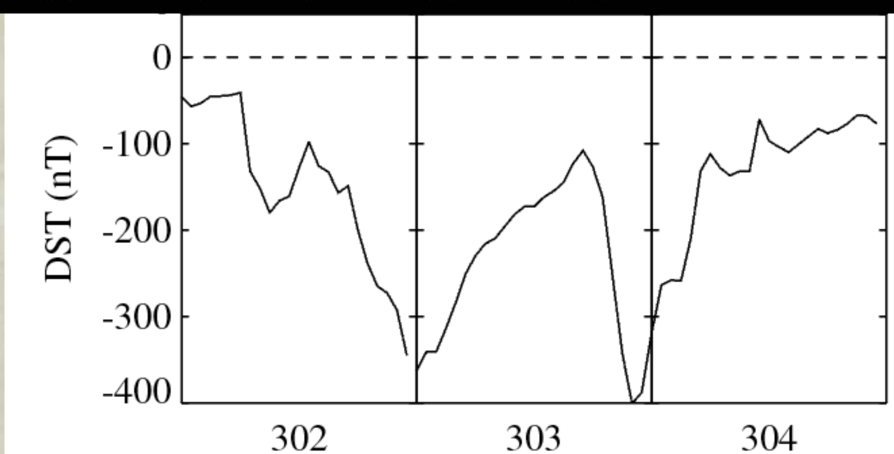

CHAMP doesn't always find the peak in density (and presumably temperature) in the low O/N2 region. This differs significantly from the GUVI finding.

Another open question : low latitude heating

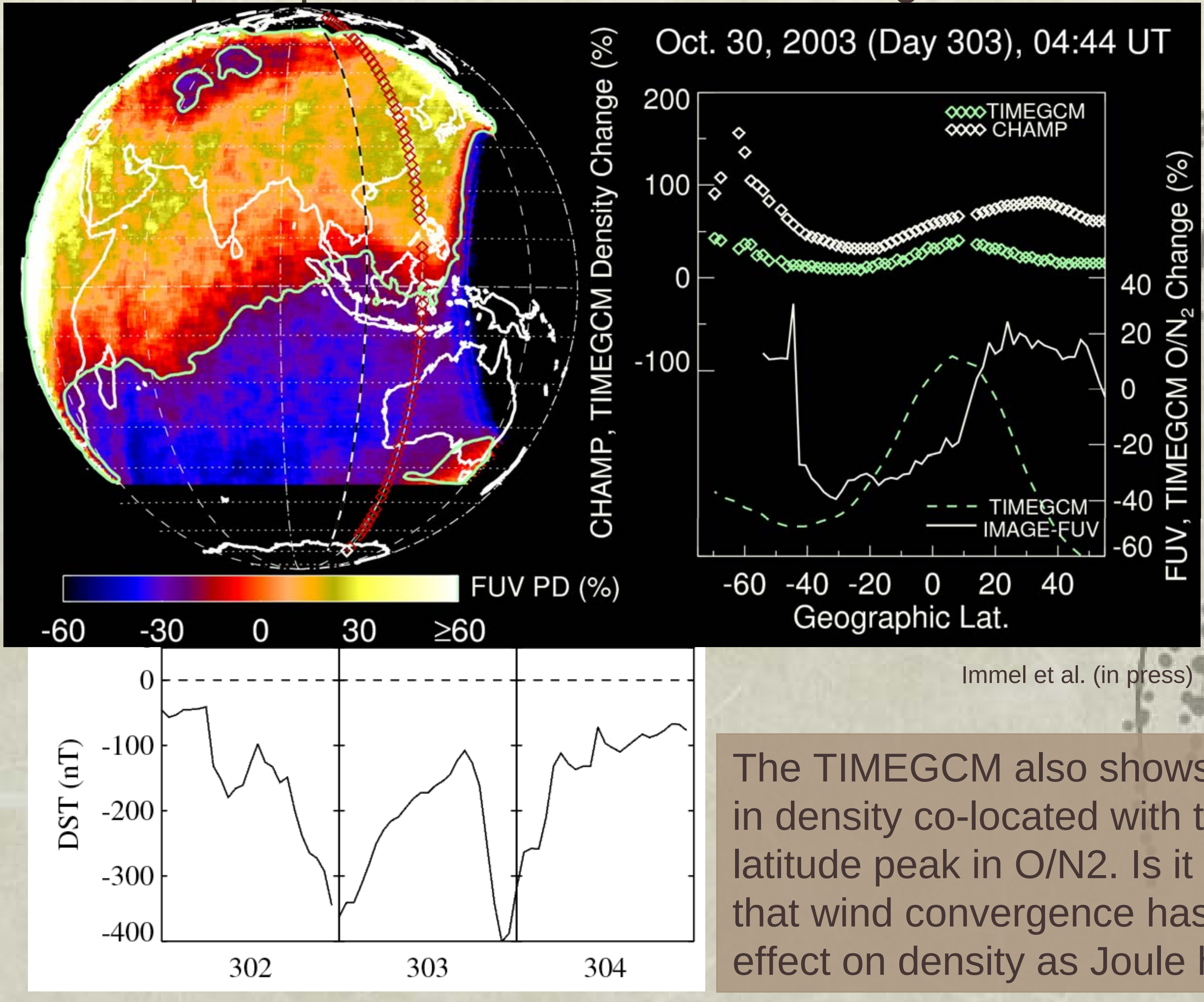

Immel et al. (in press)

The TIMEGCM also shows a peak in density co-located with the low latitude peak in O/N2. Is it possible that wind convergence has as large effect on density as Joule heating?

What about the nightside?

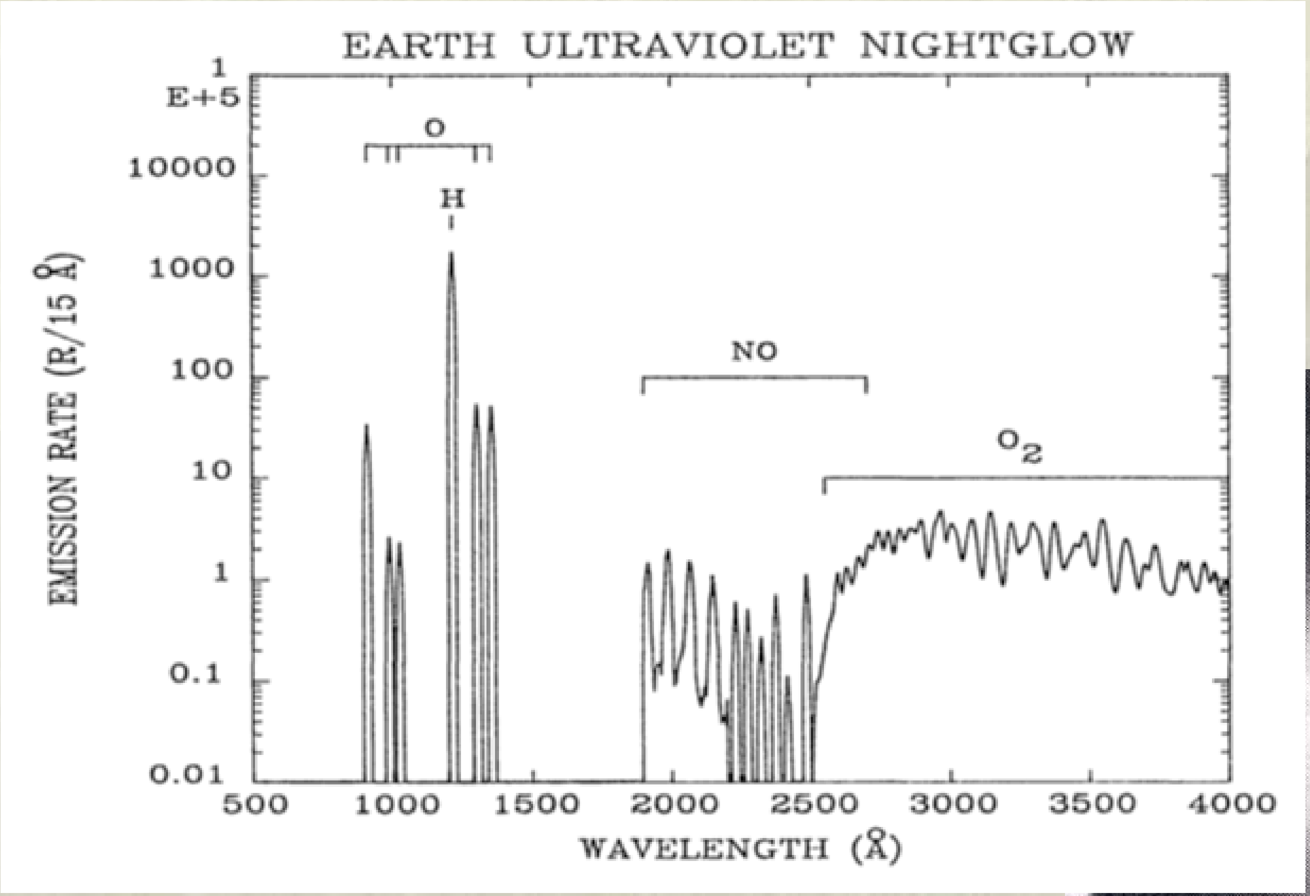

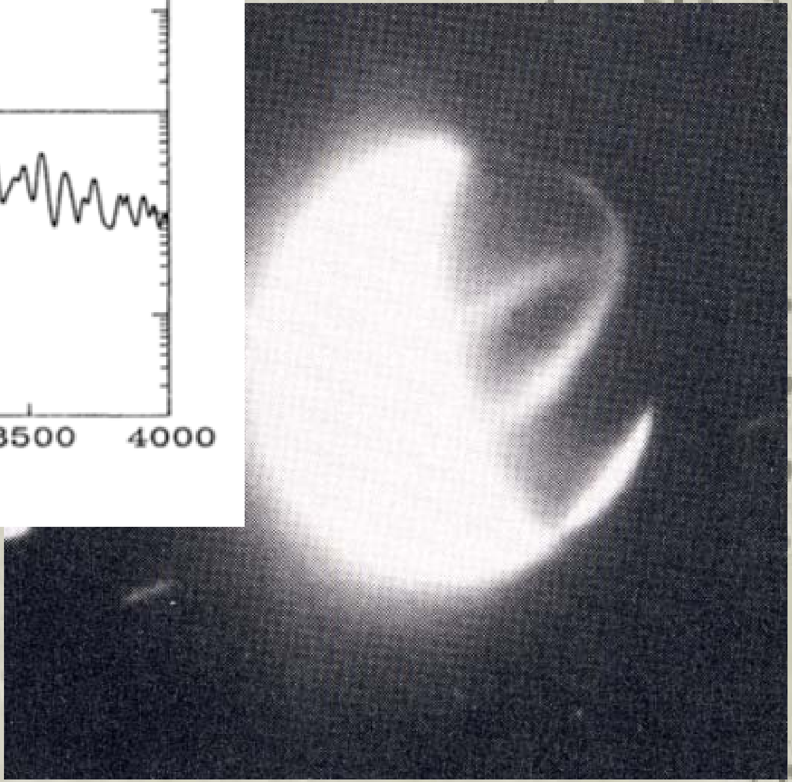

Emissions are fainter, but it depends greatly upon where you look!

Space-based imaging of the ionosphere show that it is remarkably structured and variable.

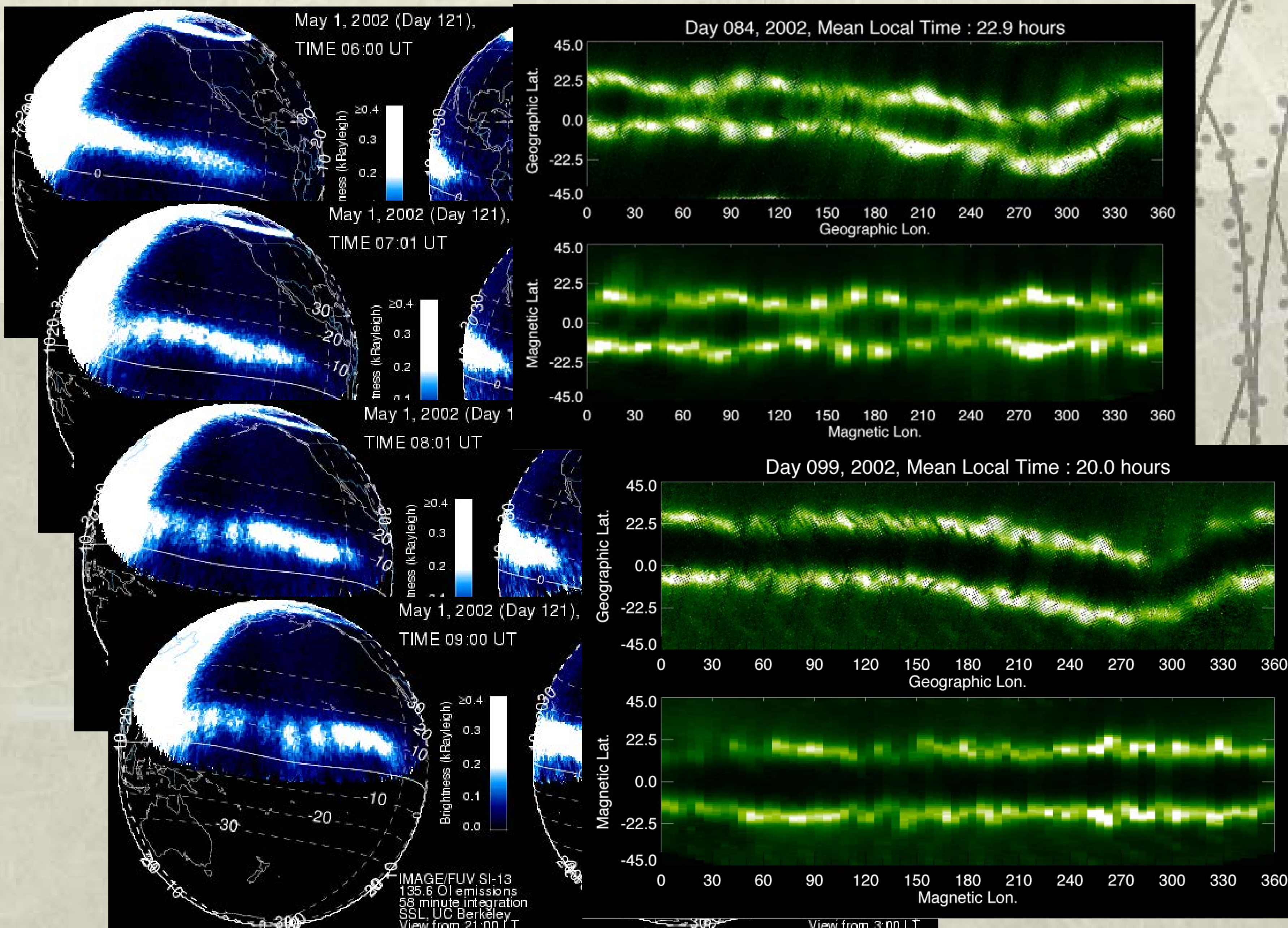

Global scale wind patterns at E-Region altitudes drive currents and electric fields throughout the daytime ionosphere

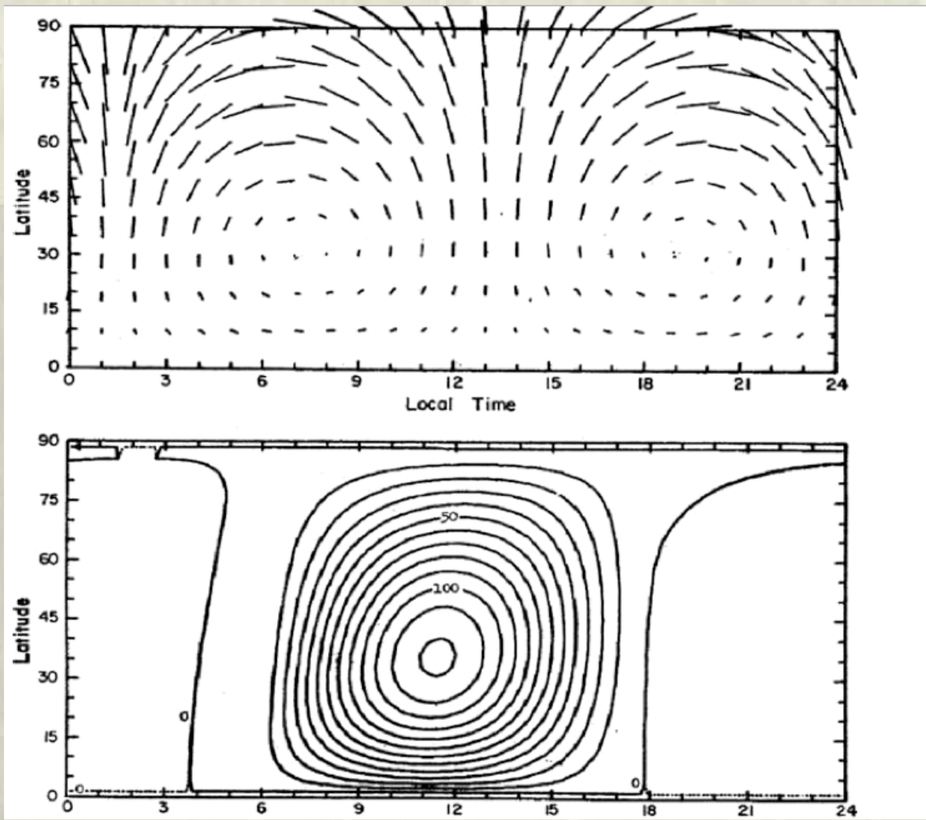

Tarpley,(1970)

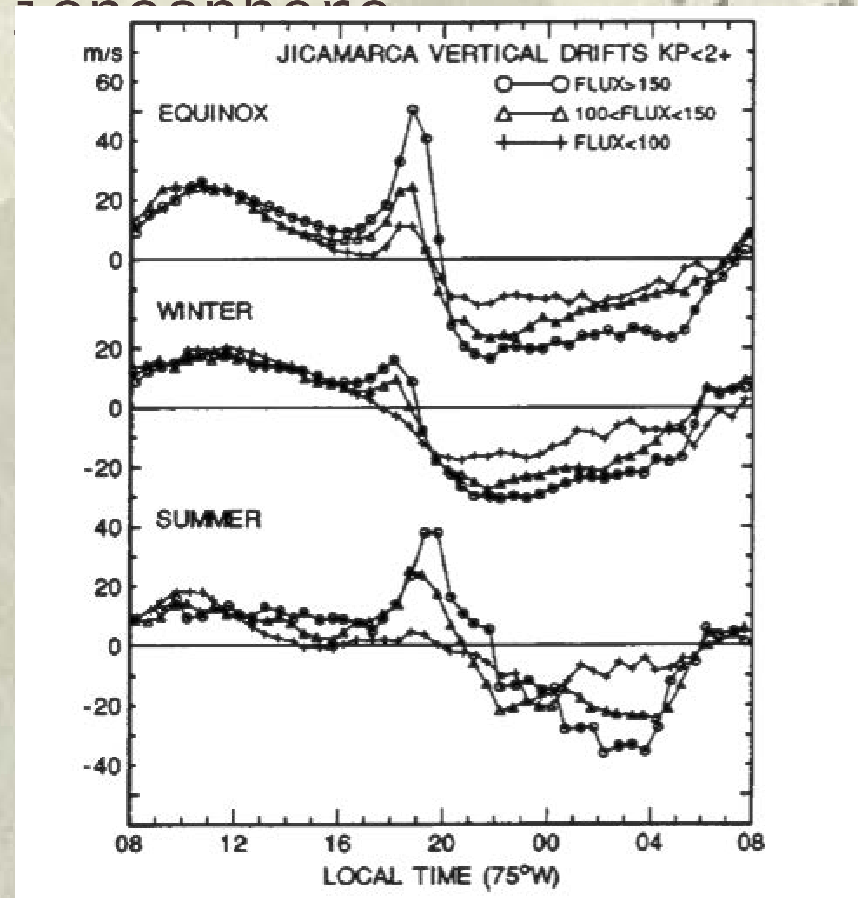

Fejer *et al*. (1991)

John Makela’s Camera System 7774 Å

Lunar Camera, 1304 Å

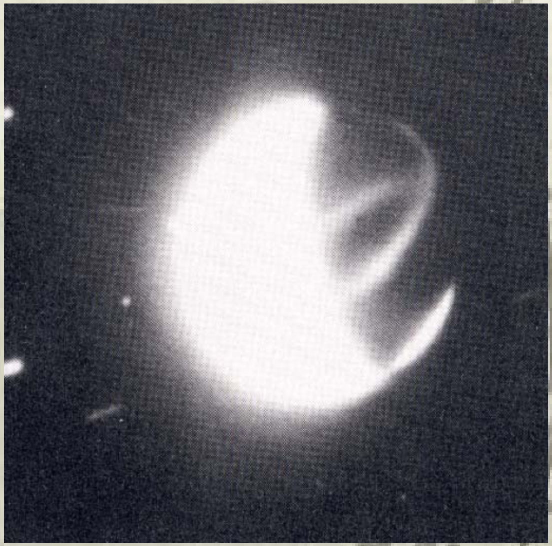

QuickTime™ and a
YUV420 codec decompressor
are needed to see this picture.

IMAGE SI13, 1356 Å

QuickTime™ and a
YUV420 codec decompressor
are needed to see this picture.

During the day, the sun provides a constant source of plasma, mainly in the form of O^+. This builds into the Equatorial Ionospheric Anomaly which rotates onto the nightside and glows at multiple

First observations of the EIA from IMAGE showed it to be reduced in density and height/latitudinal extent in particular sectors.

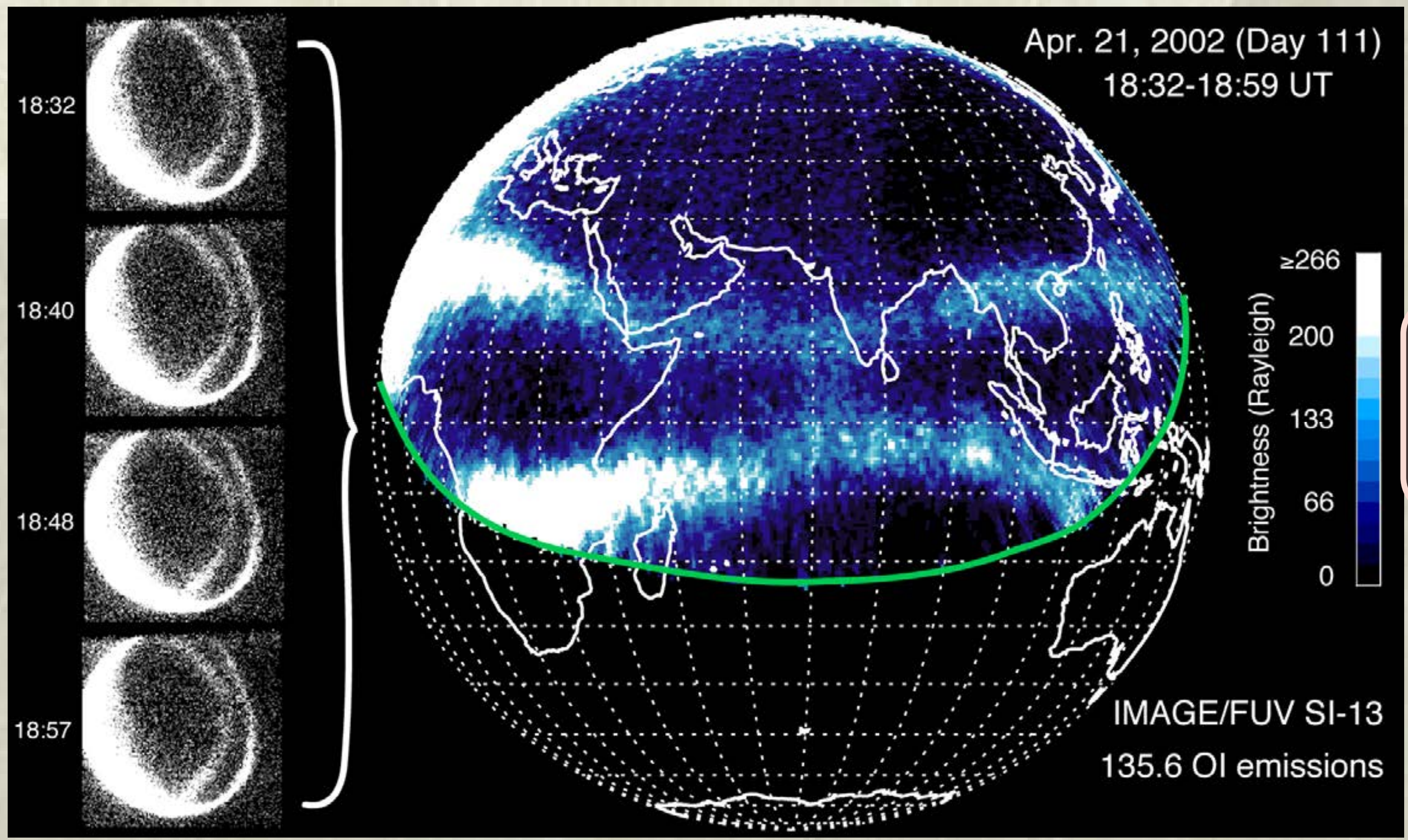

Co-variation of EIA brightness and latitude/separation

Immel et al. (2006)

TIMED-GUVI found a similar signature, and sometimes quite different from day to day.

February 2, 2002

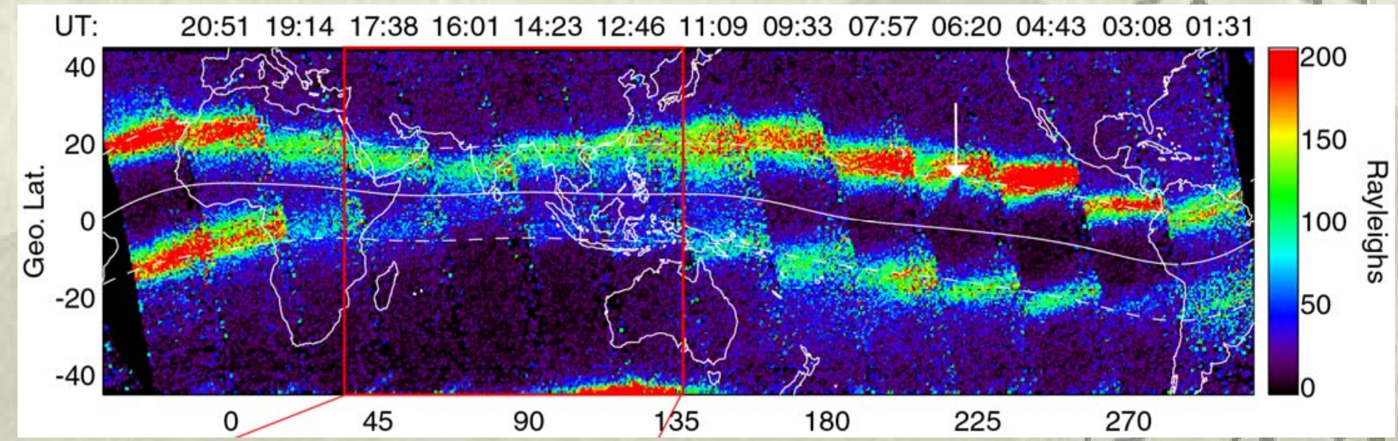

February 3, 2002

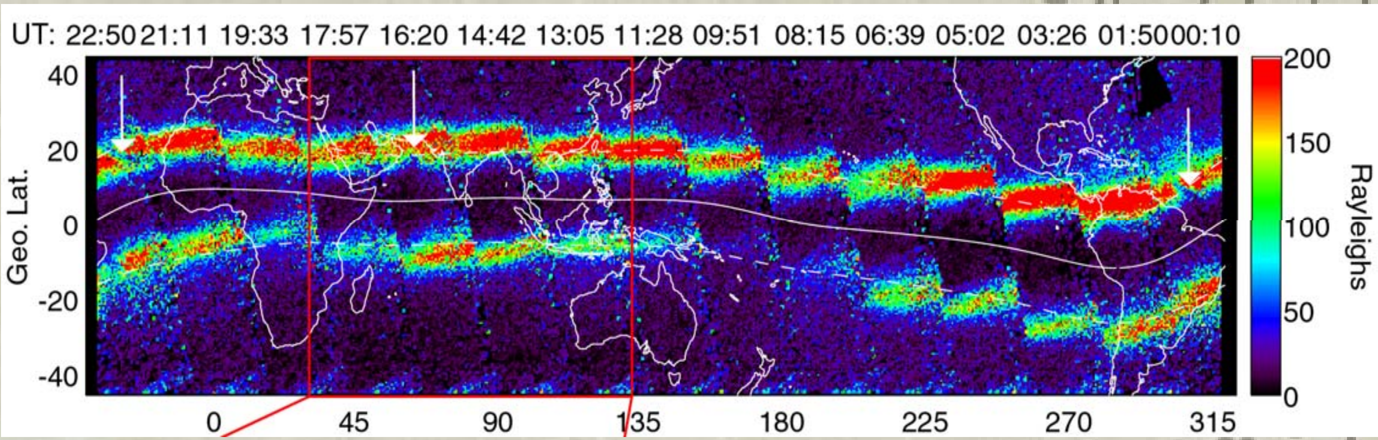

Basu et al. (in press)

Sagawa et al. [2005] found with IMAGE that this variability occurred repeatedly around the planet.

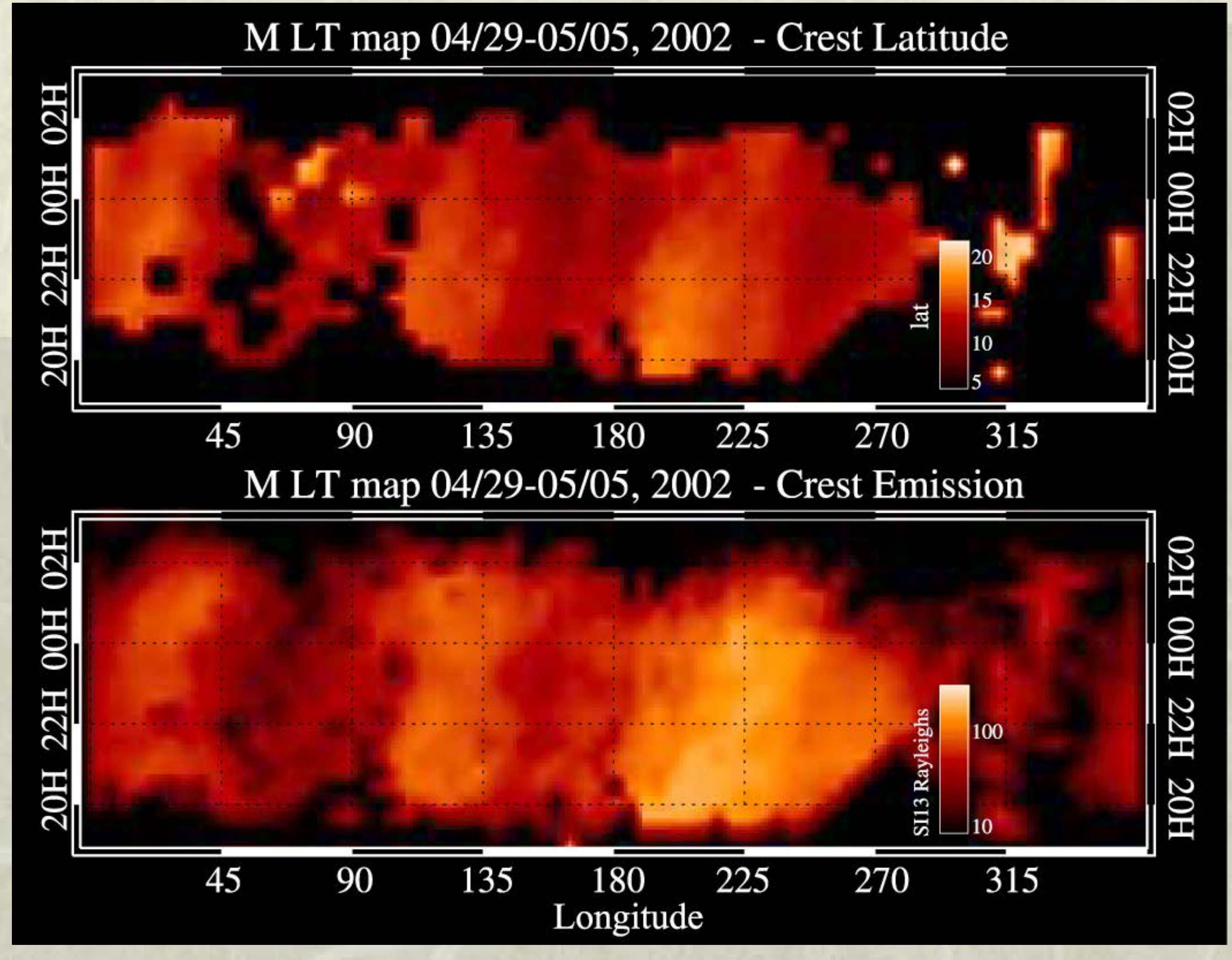

Sagawa et al. (2005)

Co-variation of EIA brightness and latitude/separation

Sagawa *et al.* [2005] noted the correspondence of the 4-peaked periodicity in the ionosphere with tides, stating:

[23] It is quite possible that the neutral wind fi[...] the nonmigrating tide causes modification to th[...] dynamo electric field, although the wind field [...] propagate up to the *F* layer. The neutral wind fiel[...] layer altitude does not have a large nonmigratin[...] nent because a tidal wave from below lose the most of its energy below 150 km, so the local heat source at the *F* layer altitude is the solar EUV which is migrating. However, because the prereversal enhancement of vertical plasma drift over the equator is controlled by both *E* layer and *F* layer dynamos, it is quite possible that the EA during the night is also affected by the *E* layer dynamo [*Millward et al.*, 2001]. It should be noted here that the development of the EA is a fairly slow process because it involves the uplift of the plasma at the geomagnetic equator and the succeeding redistribution of the plasma along field lines. We thus suggest that the nighttime EA development, which is an *F* layer phenomenon, may be controlled by the *E* layer dynamo through the prereversal enhancement of the zonal electric field. The IMAGE/FUV global observation of the EA development shows that the *F* layer plasma has a small-scale longitudinal variation, which may be related to the nonmigrating tidal component in the *E* layer neutral wind field.

dynamo through the prereversal enhancement of the zonal electric field. The IMAGE/FUV global observation of the EA development shows that the *F* layer plasma has a small-scale longitudinal variation, which may be related to the nonmigrating tidal component in the *E* layer neutral wind field.

Sagawa *et al.* referenced the recent work of Hagan and Forbes on semi-diurnal (12-hour) tides .

In 2002, and 2003, the Global Scale Wave Model was updated with a new inputs incorporating latent heat forcing originating in deep tropical convection.

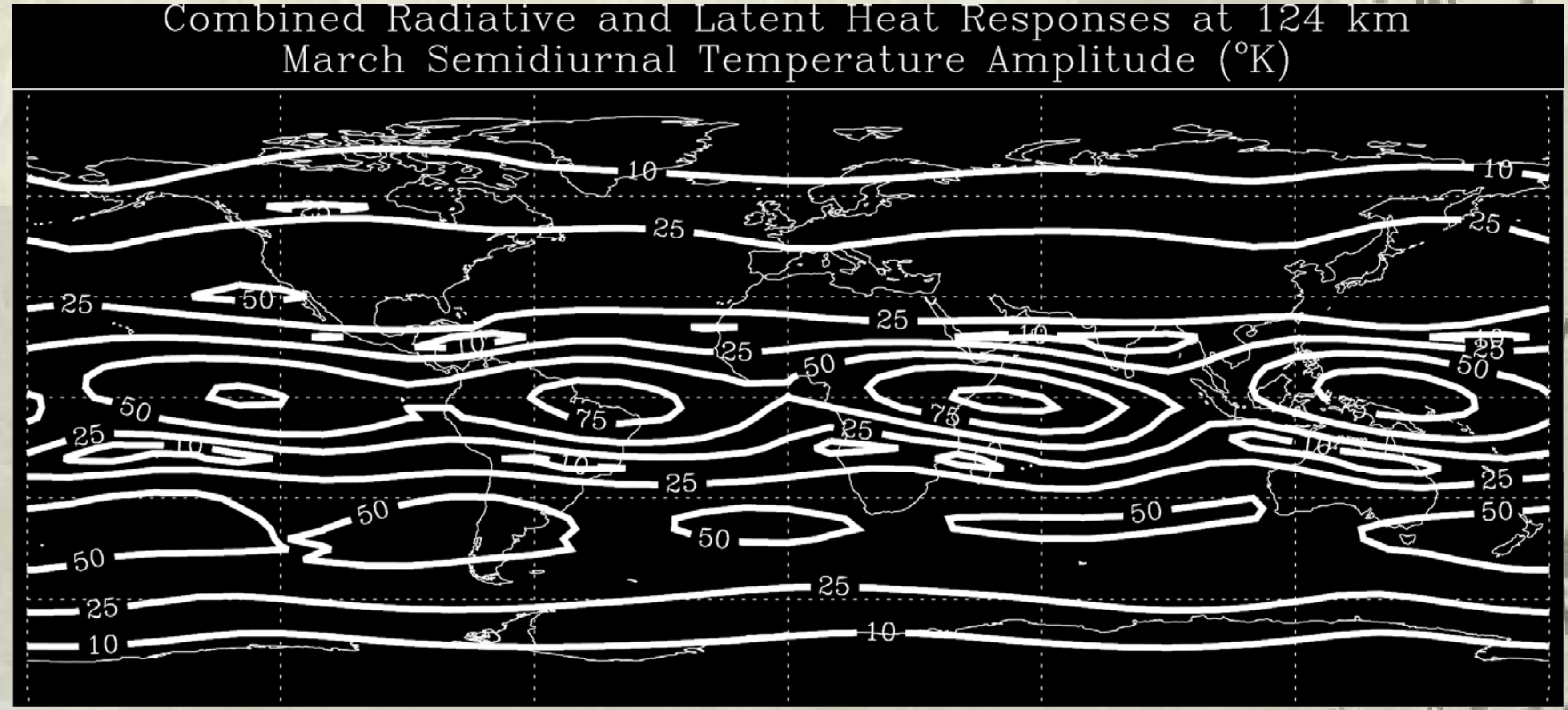

Hagan and Forbes (2003)

Energy and momentum propagating upward energize the tidal motion of the atmosphere, in a main migrating component (W1) and a similarly strong E3 wave.

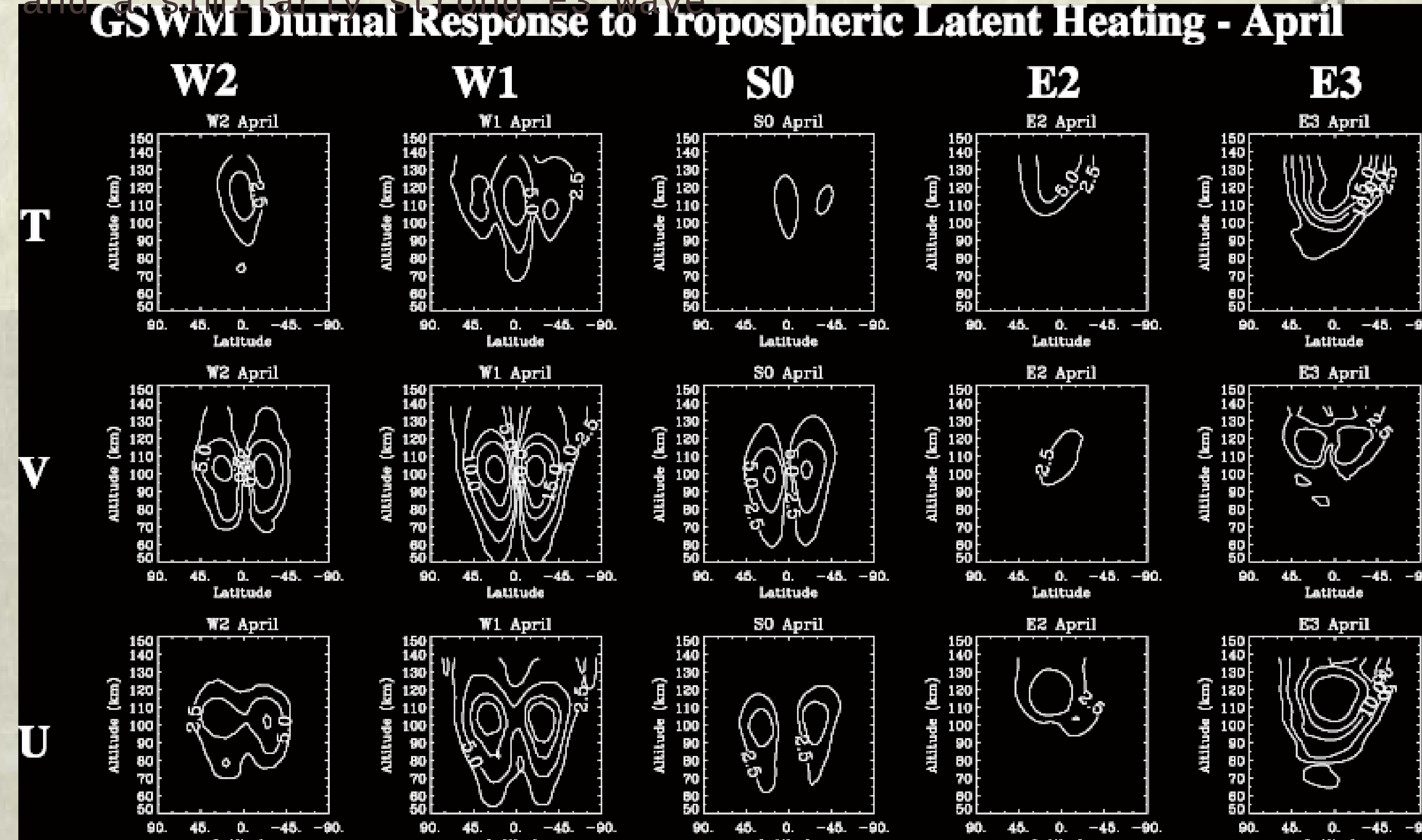

The eastward propagating waves reach maximum amplitudes in the E-region and extend well above.

TIMED-GUVI:3-day average

IMAGE-FUV:30-day average

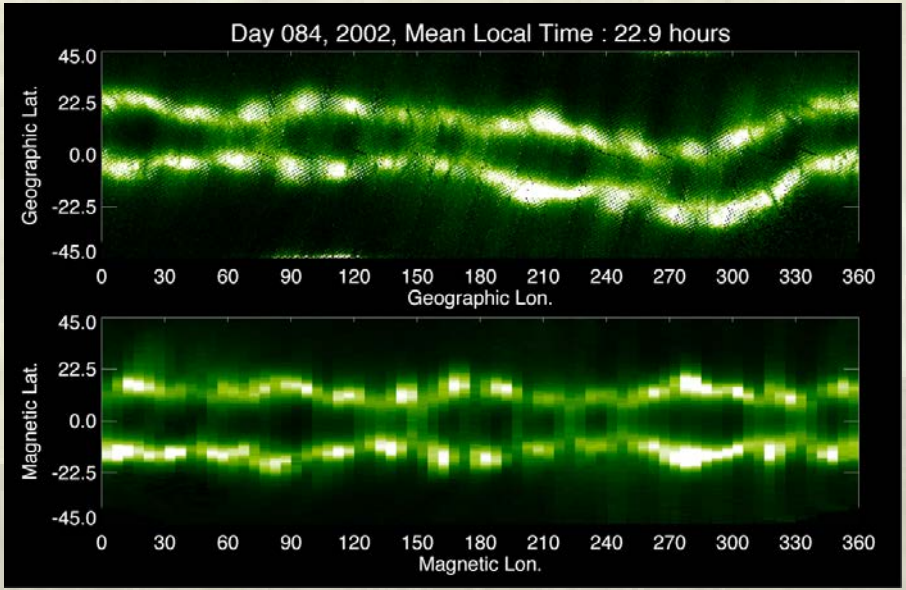

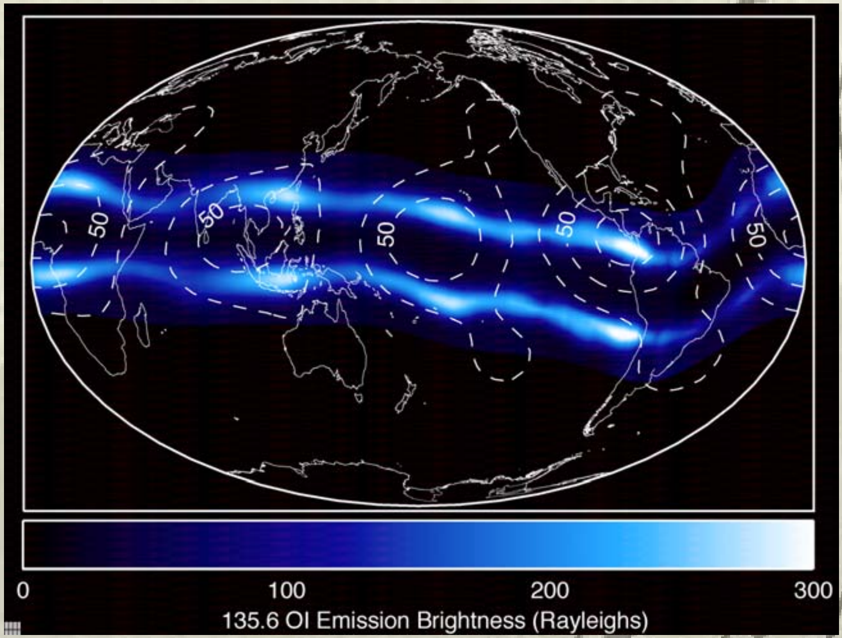

After some initial analyses of the FUV data, it became clear that the equatorial ionospheric anomaly varied in a manner that directly corresponded to recent results showing large variation of tidal winds and temperatures in the E-region around Earth.

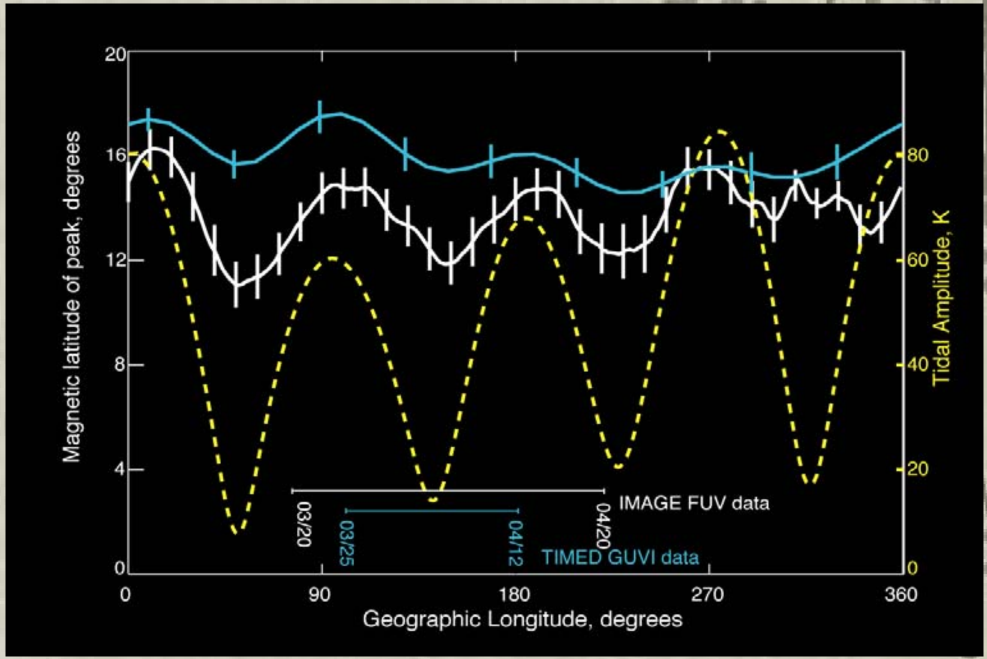

Seasonal Ionospheric, Tidal Variability

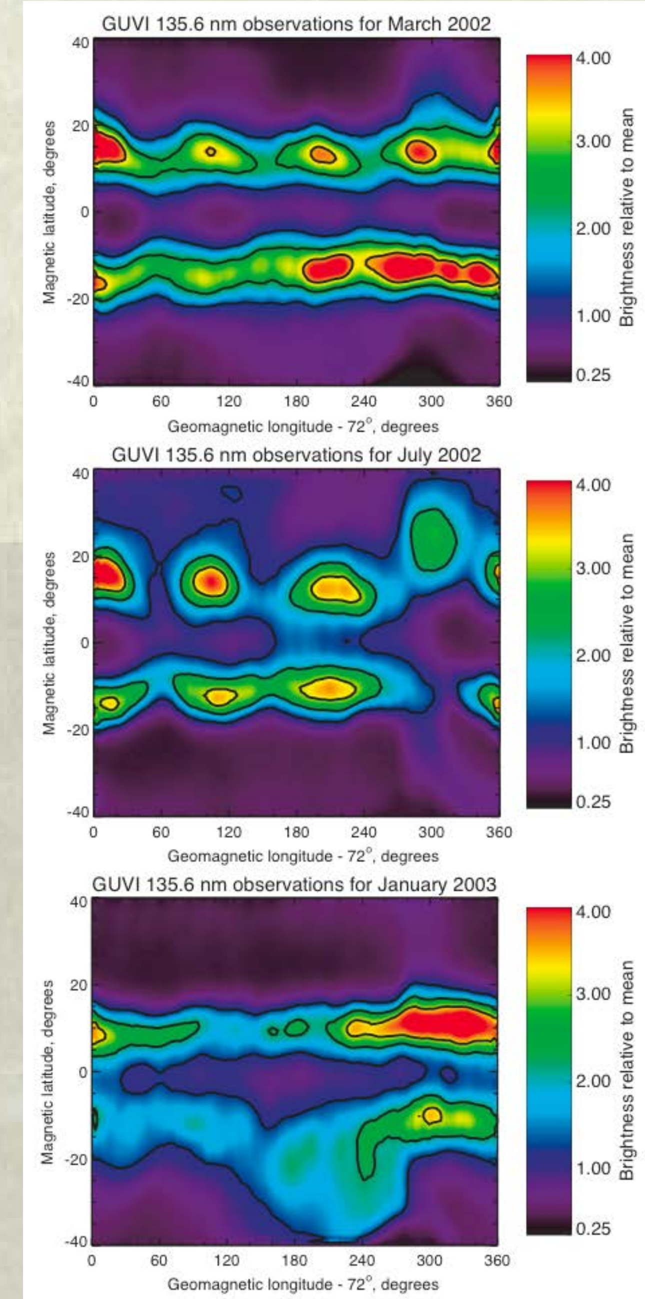

England et al., in press

Amplitude of the DE-3 tide in 2003

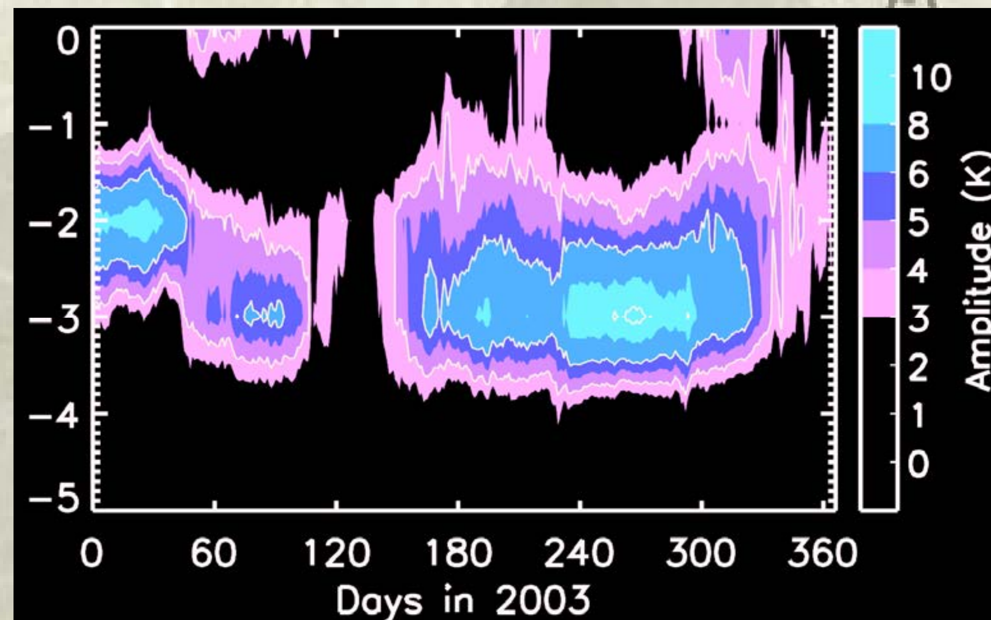

Forbes et al. (2008)

Apart from effects driven by other sources (e.g., seasonally dependent interhemispheric winds) major changes in EIA morphology can apparently be attributed to changes in tides, here measured by TIMED-SABER.

Wave Power in GUVI EIA

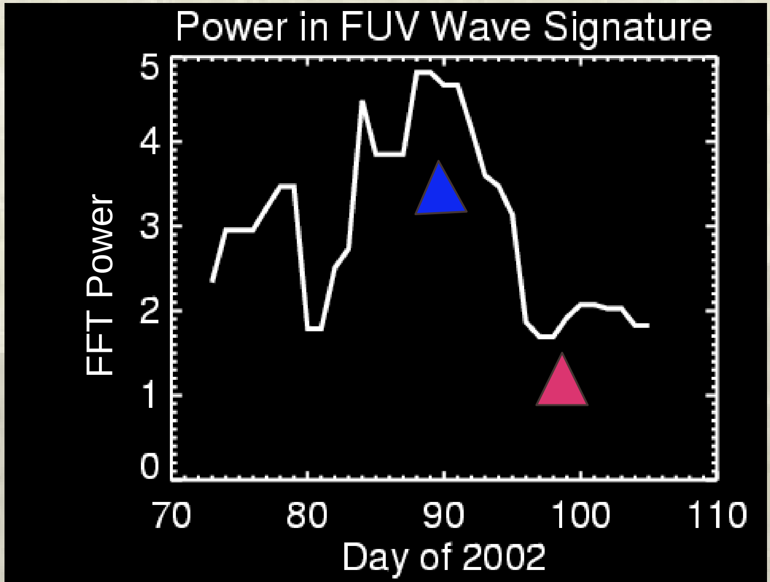

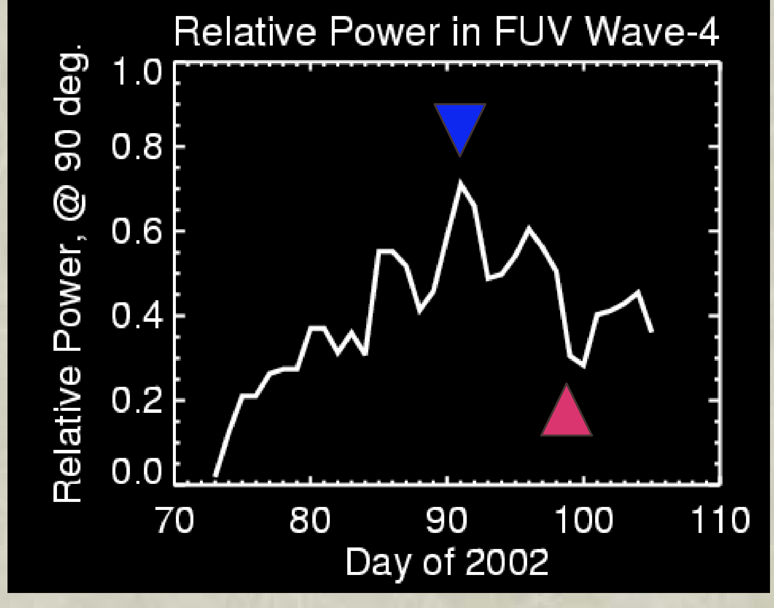

3-day GUVI averages of EIA brightness

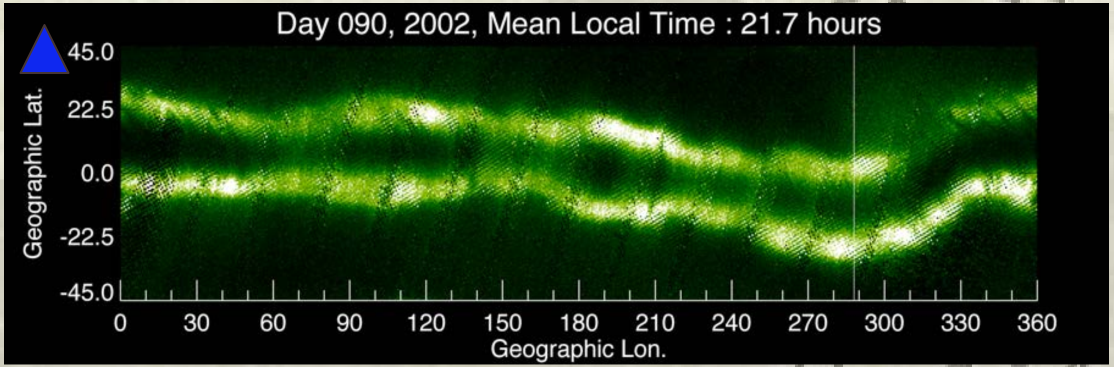

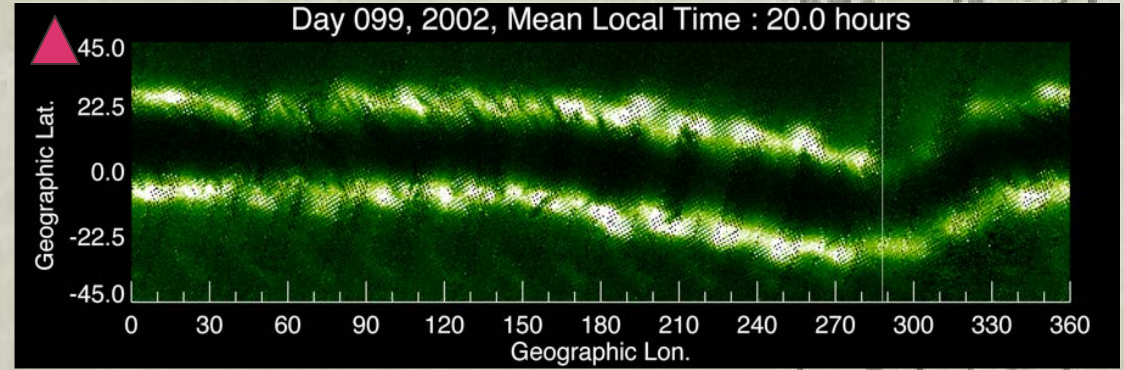

The monthly and weekly variability in the global morpology of the EIA can be quantified by the use of a Fourier transform

Wave Power in E-region Temperatures

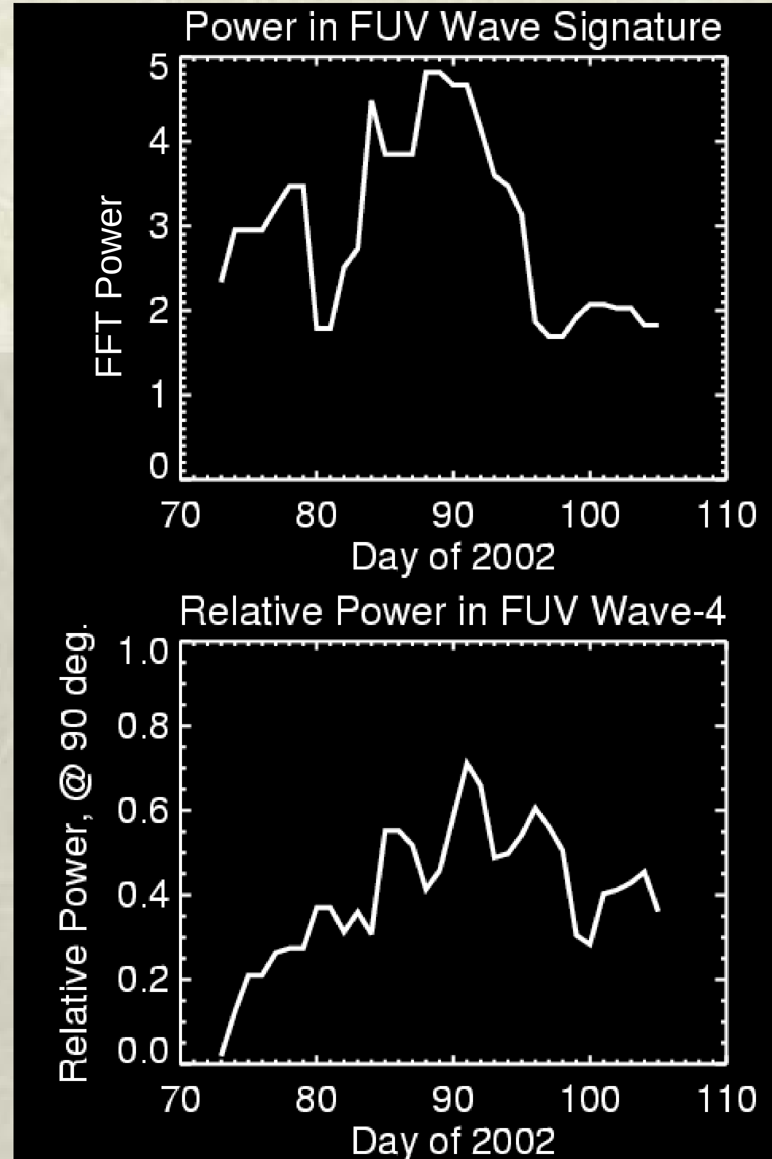

SABER Equatorial Temp. Residuals

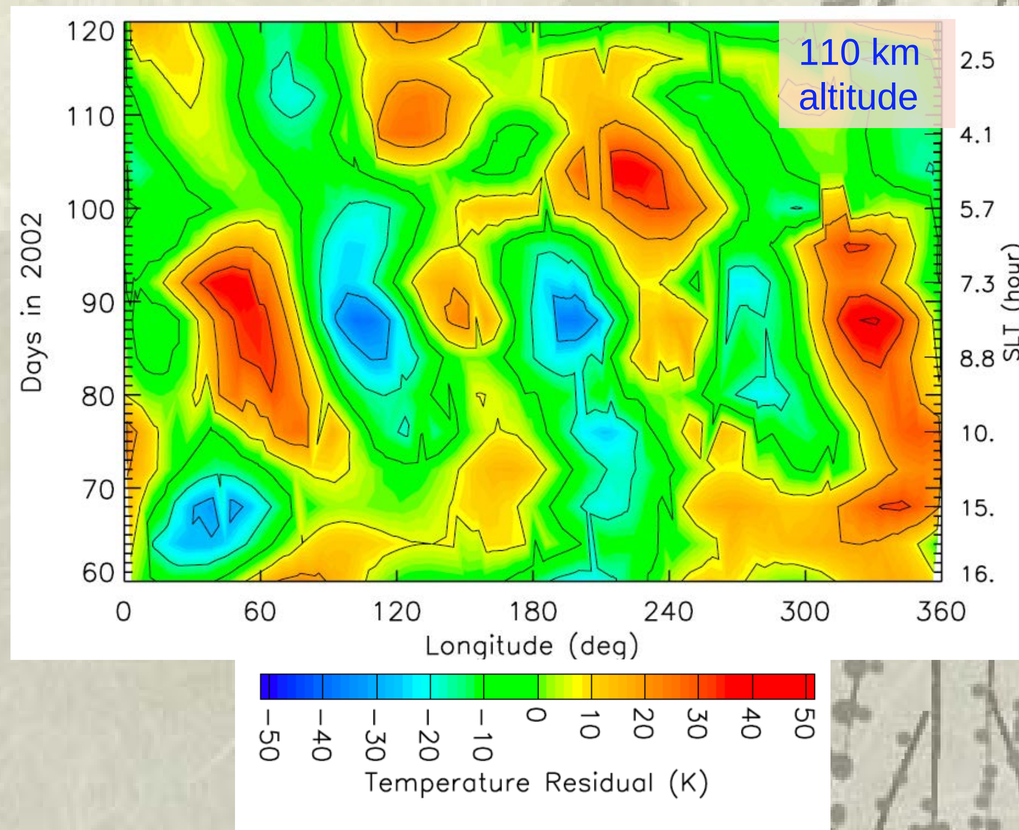

A similar analysis of SABER temperatures shows that the wave-4 signature in E-region temperatures and F-region densities covary.

Wave Power in GUVI EIA

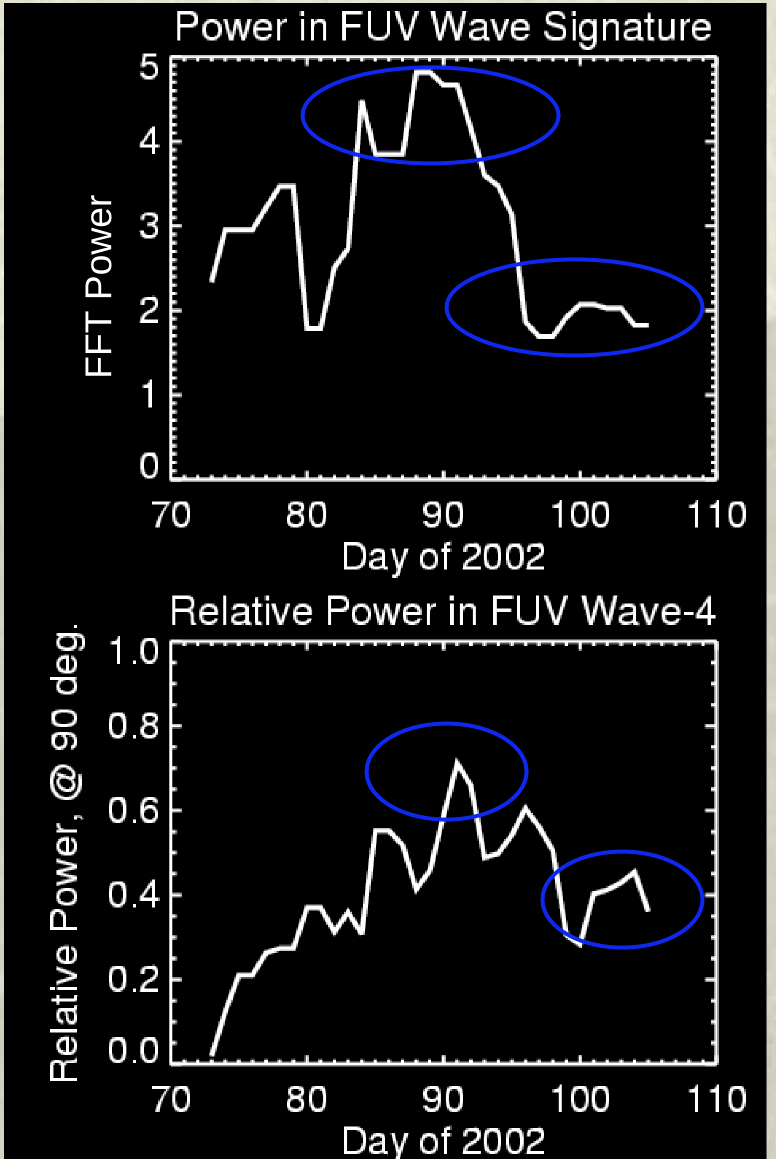

Wave Power in SABER Temps.

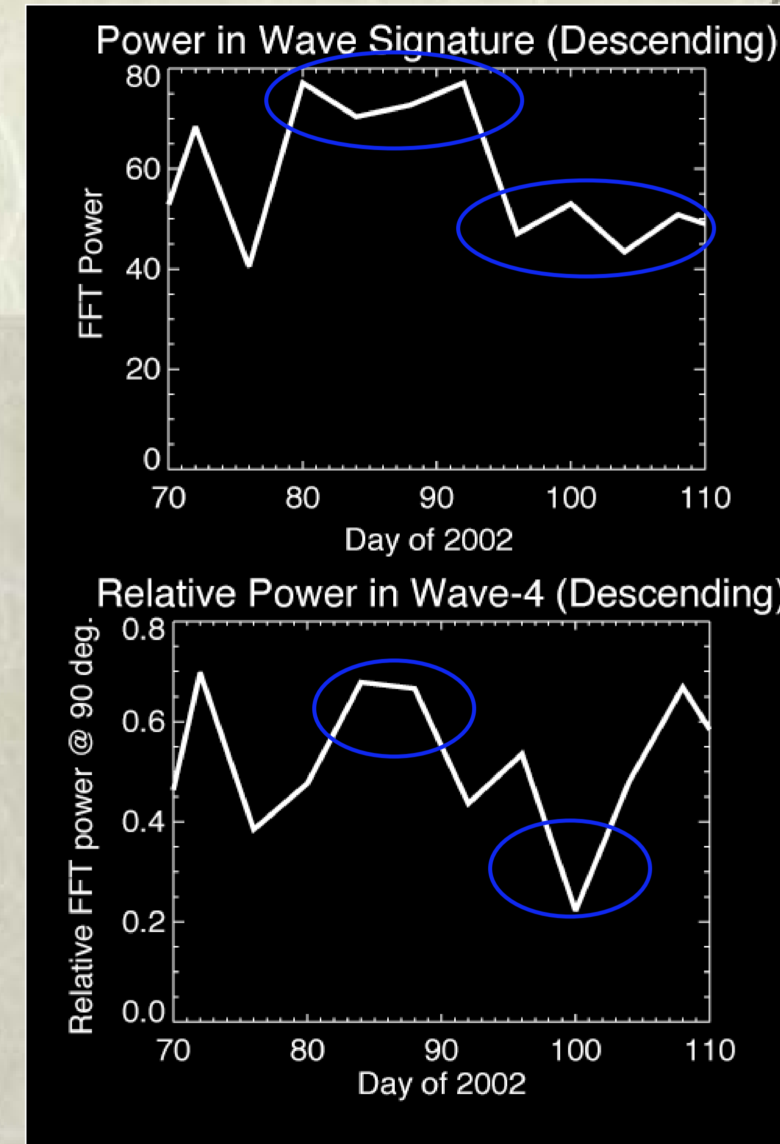

Immel et al. (in press)

One more open question: 6.5 day wave

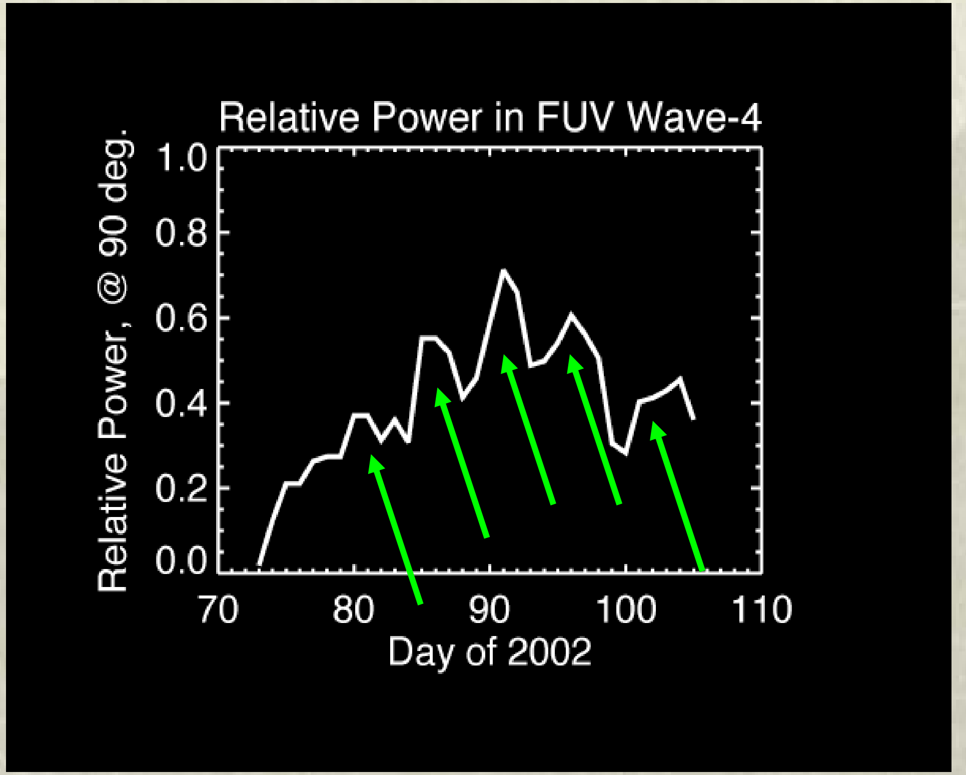

Is the apparent periodicity in wave-4 power indicative of modification of the upward propagating tides by the 6.5-day planetary wave?

Where have these tides been all my life?

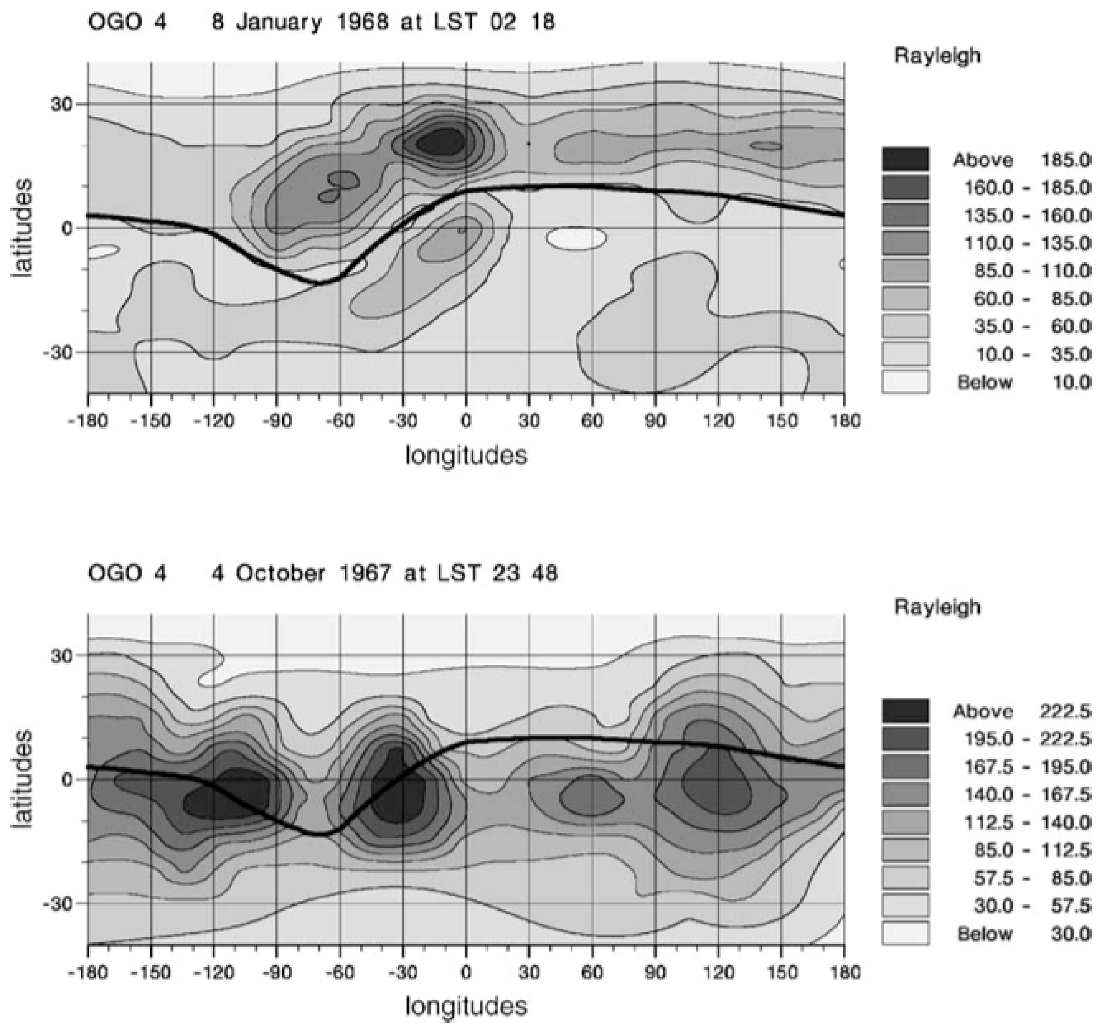

Fig. 1. Zenith emission lines (Rayleigh) shown as a function of latitudes and longitudes observed by the Orbital Geophysical Observatory (OGO 4). The black line is the magnetic equator. 8 January 1968 (top), 4 October 1967 (bottom).

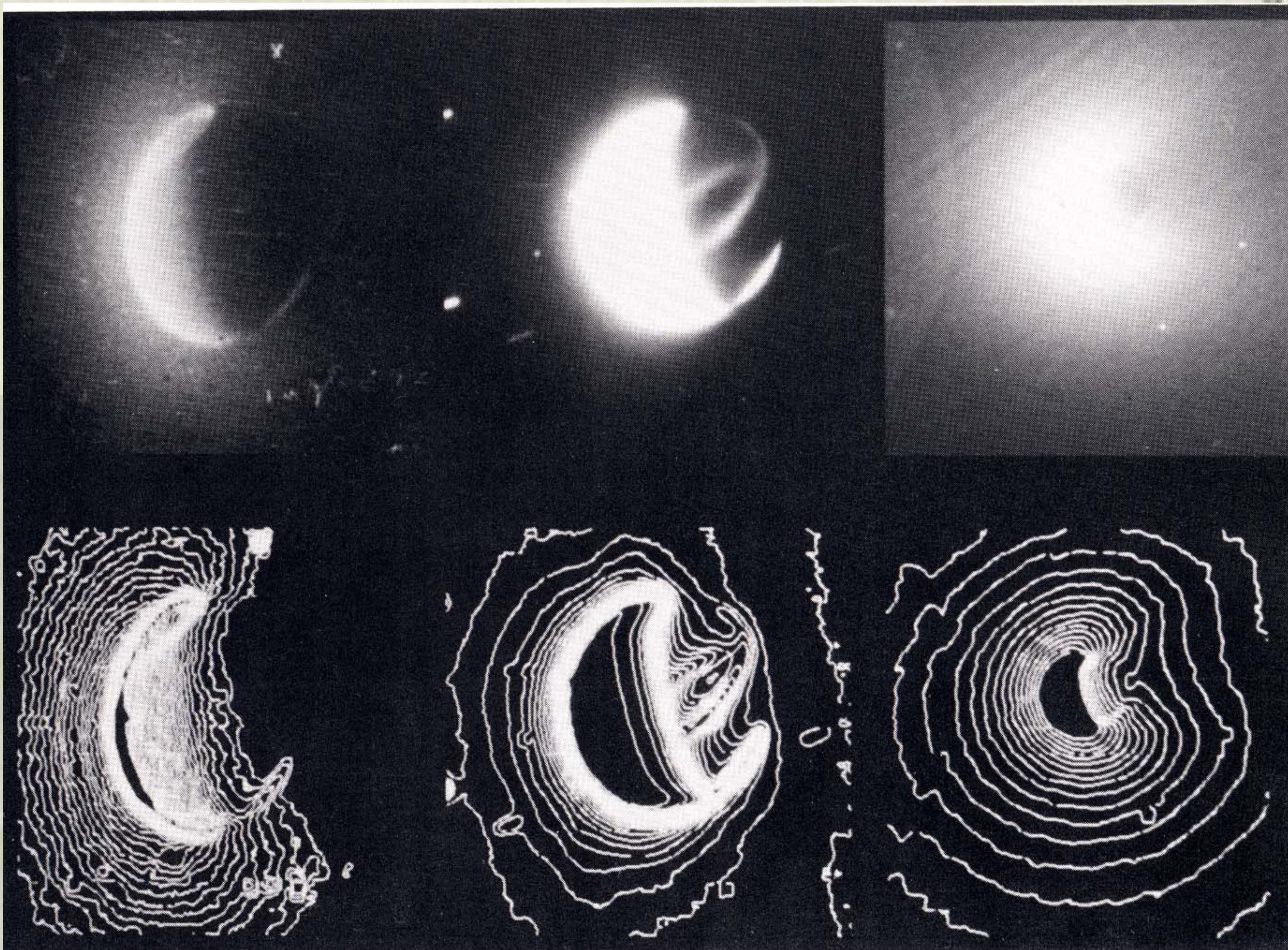

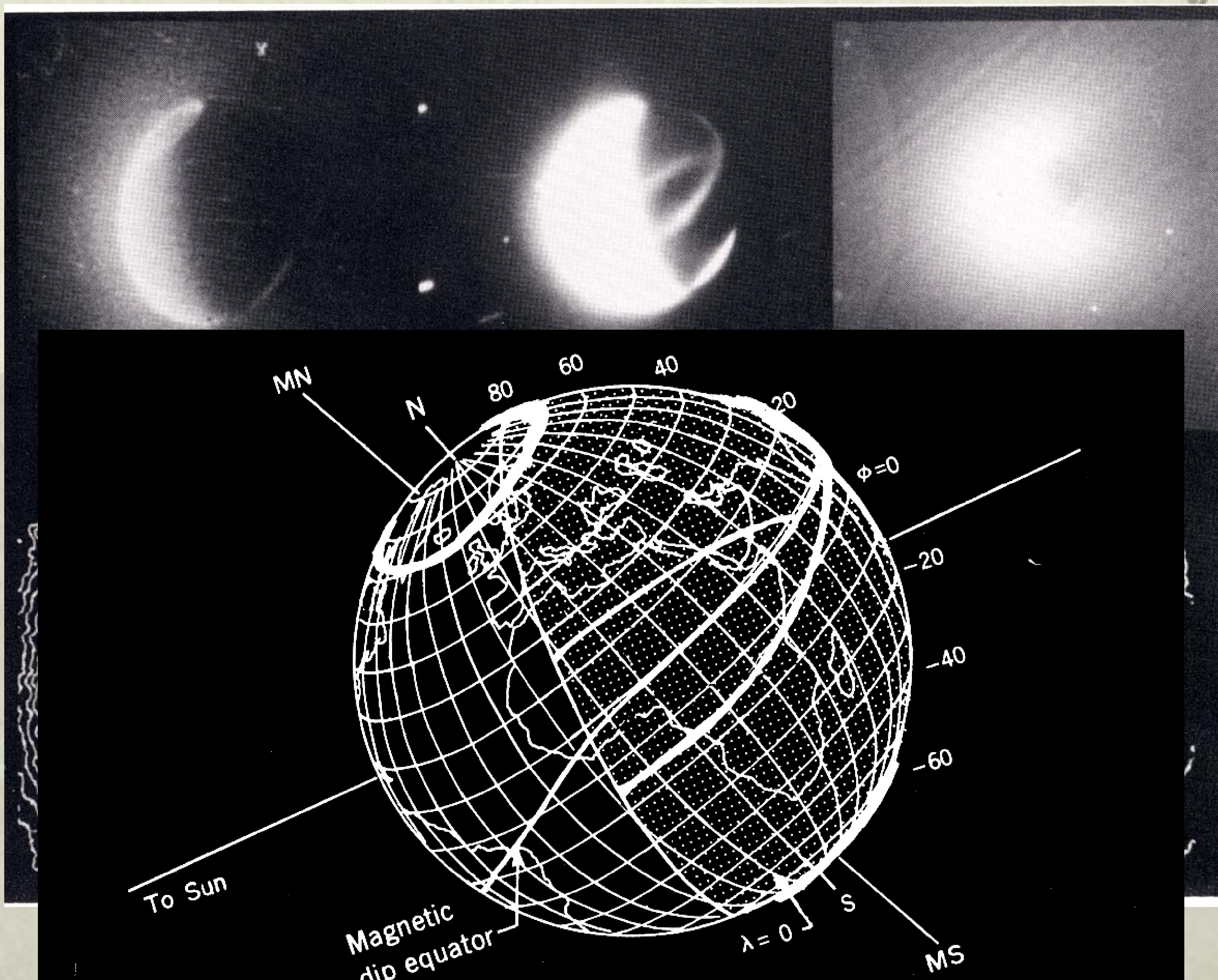
MN
N
80
60
40
20
φ =0
-20
-40
-60
To Sun
Magnetic
dip equator
λ = 0
S
MS

Thank you for your attention!